UNIVERSITÀ DI PARMA

UNIVERSITA' DEGLI STUDI DI PARMA

DOTTORATO DI RICERCA IN MEDICINA MOLECOLARE

CICLO 35°

in CO-TUTELA con VALL D'HEBRON INSTITUTE OF ONCOLOGY

PRE-CLINICAL AND CLINICAL VALIDATION OF RAD51 AS A FUNCTIONAL AND DYNAMIC BIOMARKER OF DNA REPAIR DEFICIENCY BY HOMOLOGOUS RECOMBINATION

Coordinatore:
Chiar.mo Prof. Prisco Mirandola

Tutore:
Chiar.mo Prof. Antonino Musolino

Co-tutore:
Dr.ssa Violeta Serra

Dottorando: Benedetta Pellegrino

Anni Accademici 2019/2020 – 2021/2022

1. Introduction

1.1. Homologous Recombination Repair Pathway

Homologous recombination repair (HRR) is an error-free mechanism of DNA repair that restores the genomic sequence of broken DNA ends using the sister chromatid as a template[1]. HRR is crucial during DNA replication to restore DNA double-strand breaks (DSBs) before meiosis[2]. Indeed, DSBs are the most dangerous type of DNA damage, as the integrity of both chromatids is simultaneously compromised[2]. For this reason, eukaryotes have developed sophisticated and highly organized processes to respond to DNA damage, such as HRR[3]. When HRR pathway functionality is defective, more imprecise mechanisms of DSBs repair (i.e. Non Homologous End Joining, NHEJ) are activated which tend to make mistakes, generating chromosomal deletions or translocations[1] (**Figure 1**).

HRR repairs DSBs during S and G2 phases of the cell cycle, when the intact sister chromatid is available and serves as a template for DNA damage restoration[1]. ATM and ATR (ataxia telangiectasia and Rad3-related) kinases reveal the presence of DSBs, activating signals mediator like CHK2 and BRCA1; the effectors of the cascade are BRCA2 and RAD51 [2](**Figure 1**). HRR also includes other genes that contribute to the DNA damage response, such as PALB2 and BRIP1[2].

In detail, the HRR pathway involves:

- Sensors, i.e. elements that are able to detect damaged DNA ends. In response to DSBs or to collapse of the replication fork, sensors detect damage and signal mediators, recruit or activate effectors that repair DNA damage, and activate cell cycle checkpoints [2] (**Figure 1**). The main sensor of HRR is γH2AX, which is phosphorylated in the presence of DSBs and forms nuclear foci.
- Mediators, i.e. elements that facilitate the interaction between sensors and effectors. The key mediators are RAD50, ATM (which phosphorylates CHECK2), ATR (which phosphorylates CHECK1) and BRCA1 [3].

- Effectors, i.e. elements that perform DNA repair. RAD51 recombinase is the enzyme ultimately involved in DNA repair[3]. RAD51 is recruited, through BRCA2, to replace RPA coated onto ssDNA [3]. In the presence of ATP, RAD51 is capable of forming nucleoprotein strands with DNA[3].

An impairment in the HRR pathway is also known as HRR deficiency (HRD). Tumors harboring HRD are called HRR-deficient tumors and account for 17.4% of all tumors[4]. Tumors with the highest prevalence of HRD are breast cancers (BC) (16-22% of cases), with a pick in Triple Negative BC (TNBC) (40-70%)[5], and high-grade serous ovarian cancer (HGSOC) (about 50%)[6].

1.2. Defective DNA repair as a therapeutic target: synthetic lethality

PARP inhibitors (PARPi) are drugs particularly active in tumors harboring HRD. Synthetic lethality was the first mechanism of action of PARPi to be identified.

Synthetic lethality occurs when, considering two genes, if a perturbation (e.g. a mutation) is found in only one of the two genes is still sustainable, but if it occurs simultaneously in both genes, it becomes lethal (**Figure 2**)[7].

Synthetic lethality is a useful approach that can be exploited to detect biological mechanisms of normal and cancerous cells, but also to administer tailored treatments: the interaction between poly(ADP-ribose) polymerase (PARP), and BRCA1 and BRCA2 (BRCA1/2) genes is exploited through the use of PARP-inhibitors (PARPi), which induce synthetic lethality in germline BRCA1/2 (gBRCA1/2)-mutated tumors[7, 8].

PARP1 and PARP2 (poly(ADP-ribose) polymerase 1 and 2) play a key role in repairing Single Stranded Breaks (SSBs): they are DNA damage sensors and signal transducers that operate through the synthesis of negatively charged polyADP-ribose chains (PARylation) on target proteins as a form of post-translational modification[8]. PARP1 can eventually PARylate itself, resulting in self-

PARylation[8]. PARP1 binds damaged DNA at single-strand breaks (SSBs), resulting in allosteric modification in its structure (PARylation) and activation of its catalytic function[8].

Recent findings indicate that a major mechanism by which PARPi kill cancer cells is by trapping PARP1 and PARP2 to the sites of DNA damage[9]. The PARP enzyme-inhibitor complex "locks" onto damaged DNA and prevents DNA repair, replication, and transcription, leading to cell death[9]. Several clinical-stage PARPi, including veliparib, rucaparib, olaparib, niraparib, and talazoparib, have been evaluated for their PARP-trapping activity. Although they display similar capacity to inhibit PARP catalytic activity, their relative abilities to trap PARP differ by several orders of magnitude, with the ability to trap PARP closely correlating with each drug's ability to kill cancer cells[9].

1.3. Biomarkers of HRD

PARPi and platinum salts induce DSBs DNA damage, thus being particularly active in HRD tumors like germline BRCA1/2 (gBRCA1/2)-mutated HGSOC and BC patients. HRD could be due to loss-of-function mutations in HRR genes, such as BRCA1, BRCA2, RAD51C, RAD51D or PALB, due to gene promoter hypermethylation (with consequent reduction of its expression) of HRR genes; or to causes that are still to be determined[10]. Therefore, there is an urgent need to identify HRD-tumors, beyond those described, that may also benefit from PARPi and platinum salts.

Alterations in HRR genes

Germline mutations in BRCA1/2 genes are implicated in the onset of 13-15% of HGSOC and 15% of TNBC and are associated with the “Hereditary Breast and Ovarian Cancer Syndrome (HBOCS)” [11]. Tumors arising in individuals harboring gBRCA1/2 mutations are frequently characterized by a somatic loss-of-function aberration of the corresponding wild-type BRCA1/2 allele and, therefore, HRD. Several randomized clinical trials have shown that gBRCA1/2-mutated HGSOC benefit from

PARPi maintenance treatment and that gBRCA1/2-mutated BC are sensitive to PARPi and platinum salts[12].

BRCA1/2 somatic mutations occur in 5-7% of HGSOC and 3% TNBC, respectively[13, 14]. In HGSOC, clinical outcomes of patients with sBRCA1/2 mutations are similar to those of patients with gBRCA in terms of progression-free survival (PFS)[13]; in mTNBC, the magnitude of benefit from PARPi and platinum salts seem to be slightly lower in patients harboring sBRCA1/2 mutations than gBRCA1/2-mutated patients[15, 16].

In HGSOC and TNBC, clinical studies have demonstrated that somatic and/or germline mutations in non-BRCA1/2 HRR genes, such as RAD51C, RAD51D, BRIP1, ATM, CHEK1, CHEK2, and CDK12, confer an advantage in terms of ORR, when treated with PARPi, compared to WT patients[13, 16]. Overall, the benefit seems to be gene-specific and the magnitude of benefit correlates with the level of LOH[13, 16].

The clinical relevance of promoter methylation of the HRR genes is difficult to interpret. The most common hypermethylation occurs in the promoters of BRCA1 and it has been associated with HRD in preclinical models[10]. Clinical trials evaluating methylation of BRCA1, however, have yielded conflicting results, making unclear its predictive value of response to PARPi and platinum salts[15, 17, 18].

Gene scar/signature

Cancer cells and cells with BRCA1/2 mutations are characterized by genomic instability: they exhibit abnormal copy number profiles and numerous somatic mutations in the genome, including single base substitutions (SBS) and structural variants (structural variants, SVs). The evaluation of these genomic characteristics allows to identify tumors with a history of HRD, regardless of the underlying etiology.

Copy number based 'scar' assays. Genomic HRD tests have been developed using SNP based microarray technologies, measuring somatic copy number variation (CNV). In 2012, three studies reported SNP-based CNV tests that predicted BRCA status by quantifying large scale transitions (LST), loss of heterozygosity (LOH), and/or number of sub-chromosomal regions with allelic imbalance extending to the telomere (TAI)[19].

Two commercial genomic scar assays have been approved by FDA and tested to identify tumors with HRD. The "myChoice HRD" assay by Myriad tests for the presence of loss of heterozygosity (LOH), telomeric allelic imbalance (TAI), and large-scale state transitions (LST) across the genome[20]. The readout of this assay is presented as an "HRD score": a tumor with an HRD score ≥42 is labelled as HRD-positive. The "FoundationFocus™ CDx *BRCA* LOH" is designed to detect the presence of mutations in BRCA1/2 genes and the percentage of the genome affected by LOH in DNA from tumor tissue samples of patients with ovarian cancer[21]. According to the FoundationFocus test, tumors are categorized as LOH-high if score is ≥16. Finally, the non-commercial test HRDetect[17], includes additional mutational signatures characteristic patterns left on the cancer genome by each mutational process: for example, HRD has been associated with the "signature 3" described by Alexandrov et al [22].

Functional assays

A current limitation of the genomic scar assays is the impossibility to capture tumor evolution processes, such as a restoration of the HRR function in response to therapy-selective pressure. As an alternative, it could be useful to incorporate functional biomarkers based on assays capable to estimate the activity of a repair pathway in a dynamic way. A crucial step of HRR is mediated by the RAD51 protein that forms a nucleoprotein filament which is able to carry out the strand exchange step of HRR[1]. Despite some limitations yet to be solved, *in vivo* and *in vitro* studies supported the highly

sensitive and specific predictive value of lack of nuclear RAD51 foci to PARPi response[23–26]. One such limitation is that RAD51 assay may fail to identify ATM-mutated tumors that can benefit from PARPi according to their specific mechanisms of sensitivity[27–30].

1.4. Clinical implications of HRD in HGSOC and TNBC

Approximately 13% and 15% of ovarian and triple negative breast cancers (TNBC), respectively, harbor HRD that is attributable to gBRCA1/2 mutations[31, 32]. Furthermore, 50% and 40% of ovarian and TNBC, respectively, are characterized by harboring HRD in the absence of *g*BRCA1/2 mutations[5, 31]. Also, 10-12% of advanced prostate cancer harbor germline or somatic BRCA2 inactivation and up to 25% contain a DNA repair defects [33]. As HRR is required for the repair of DSBs generated during DNA interstrand cross-link (ICL) resolution, HRR-deficient tumors are sensitive to ICL-generating platinum chemotherapy[34, 35]. Moreover, BRCA1/2-mutant cells are sensitive to PARP inhibitors (PARPi), a new class of drugs that block SSB repair, favoring accumulation of DSB that HRR-deficient cells cannot repair[36]. Several PARPi have been approved for the treatment of HGSOC and BC[13, 37–40]. EMA approved olaparib as maintenance treatment for HGSOC in BRCA1/2-mutated platinum sensitive patients; rucaparib was approved for BRCA1/2-mutated patients who have already progressed to at least two lines of treatment with platinum-based chemotherapy and niraparib was labelled as maintenance treatment for patients who are in response to platinum-based chemotherapy[37, 38, 41]. Olaparib and talazoparib have been approved for BC patients with gBRCA1/2 mutations who have been previously treated with chemotherapy in the advanced setting[39–41].

In advanced HGSOC, the ARIEL2 study demonstrated the efficacy of the PARPi rucaparib as monotherapy in gBRCA1/2-mutated and/or LOH-high relapsed, platinum-sensitive HGSOC, and the ARIEL3 trial demonstrated the benefit of rucaparib as maintenance therapy in platinum-sensitive

recurrent patients who responded to platinum, regardless of the LOH status (**Table 1**)[21, 38]. The NOVA trial investigated the role of the PARPi niraparib as maintenance therapy in platinum-sensitive HGSOC population and showed that BRCA1/2-mutated and HRD-positive (according to myChoice assay) patients benefited from PARPi[13]; nevertheless, niraparib also improved PFS in BRCA1/2-WT patients with HRD-negative test, although the magnitude of benefit was smaller compared to BRCA1/2-mutated or HRD-positive patients (**Table 1**)[13]. In patients with advanced HGSOC receiving first-line standard therapy including bevacizumab, the PAOLA trial showed the addition of maintenance olaparib provided a significant PFS benefit, which was substantial in patients with HRD-positive tumors, including those without a BRCA1/2 mutation[42]. We may conclude that, in this population, genomic scars are less likely to rule out patients who benefit from PARPi, standing the high probability of response after platinum sensitivity, but the magnitude of the benefit is higher among those who are HRD-positive. Further investigations are needed to verify if an HRD test may be useful to select platinum resistant tumors that could benefit from PARPi or to identify long responders to PARPi and/or platinum salts[12].

In TNBC, several trials have investigated if genomic scars predict response to DNA-damaging agents (**Table 2**). In the neoadjuvant setting, Telli et al retrospectively assessed the predictive value of the "myChoice HRD" assay in three single-arm trials testing platinum-based therapy in the neoadjuvant setting[19]. HRD-positive patients had a higher probability to achieve a pathologic complete response (RCB 0) or to have only minimal residual disease (RCB I) after platinum chemotherapy, even among BRCA1/2 WT tumors[19]. The GeparSixto trial is a neoadjuvant study evaluating the benefit of the addition of carboplatin in HER2-positive and TNBC[5]. It showed that tumors with HRD were associated with better DFS and OS, independent of the treatment arm, but also that the addition of carboplatin was beneficial regardless of the HRD status. As this trial lacked cyclophosphamide in the

control arm, it provided data of the prognostic value of HRD in TNBC, but it may not have provided definitive word on the predictive value of HRD in relation to carboplatin. In early TNBC, considering the associated toxicity of platinums, we would conclude that there is a clinical need to dissect the role of carboplatin added to standard anthracycline-cyclophosphamide and taxane chemotherapy in HRD-positive tumors[12]. To confirm the prognostic role of this tool, a study powered to demonstrate the improvement in OS would be required. Interestingly, Litton et al have recently showed the efficacy of PARPi talazoparib in the neoadjuvant setting in BRCA1/2-mutated patients. In this setting, an HRD test could be useful to identify BRCA1/2-WT patients who can also benefit from PARPi.[43]

In metastatic TNBC, Isakoff et al conducted a phase 2 trial aimed to investigate the predictive role of genomic scars to platinum salts. Higher HRD scores were reported in responding patients independent of BRCA1/2 mutational status[44]. However, the predictive role of this HRD test was not confirmed in the TNT trial, a randomized phase 3 trial comparing the efficacy of first-line carboplatin versus docetaxel in patients with advanced TNBC[15]. According to pre-planned biomarker analysis, carboplatin resulted in higher Overall Response Rates (ORR) among patients harbouring a *g*BRCA1/2 mutation but not in subjects with other profiles associated with HRR dysfunction such as high HRD-score, BRCA1 methylation, or BRCA1 mRNA-low, all evaluated in the primary tumors[15]. These results could be partially explained by the fact that the prediction power of genomic scars tested in the primary tumor may decrease in the advanced setting because metastatic tumors may have restored the HRR function and become resistant to platinum. Again, HRD-positive tumors were more likely to respond to both chemotherapy regimens compared to the HRD-negative ones. Several open questions raised from the previous statements: first, that no data are available comparing HRD status in early and advanced breast cancer, and second, that further studies are required to dissect the role of the HRR function recovery in predicting resistance to PARPi and platinum salts[25]. Furthermore, despite the

OlympiaD and EMBRACA trials demonstrated PARPi efficacy in BRCA1/2-mutated metastatic breast cancer[39, 40], still a relevant proportion of patients did not respond and it is unknown if an HRD test would help to refine the subgroup more likely to benefit[12].

1.5. RAD51 assay as functional biomarker of HRD in early BC

The RAD51 assay was tested, retrospectively, on tumors from early TNBC patients enrolled in the GeparSixto trial[45]. From 315 participants with TNBC in the GeparSixto trial, 259 tumor samples laid on TMAs were considered suitable for biomarker analyses. 59 cases were excluded due to absence/insufficient tumor cells. RAD51, BRCA1 and yH2AX nuclear foci were successfully scored on 133/200 cores (67%)[45]. These 133 patients exhibited similar clinical and molecular characteristics to the full TNBC population (n=315) of the GeparSixto trial. Functional HRD by RAD51 (RAD51-low score) was found in 81/133 tumors (61%). The BRCA1 nuclear foci score (BRCA1 score) was low in 43% of tumors, all of them with low RAD51 values[45]. The RAD51 biomarker identified 93% (95%CI 76%-99%) of tBRCA1/2-mutated tumors and 45% (95%CI 34%-56%) of the non-tBRCA1/2 mutants as harboring functional HRD. RAD51 identified 86% of tumors with genomic HRD and 90% with genomic HRR proficiency (HRP) [45]. Overall, RAD51 and genomic HRD were 87% (95%CI 79-93%) concordant. These results demonstrated the feasibility of the RAD51 test in untreated FFPE TNBC samples and its high-degree of concordance with tBRCA1/2 mutations and genomic HRD tests[45].

The pCR in patients with RAD51-high tumors was similar between treatment arms (PMCb 31% vs PM 39%, OR=0.71, 95%CI 0.23-2.24, p=0.56) [45]. In contrast, patients with RAD51-low tumors significantly benefited from PMCb (pCR PMCb 66% vs PM 33%, OR=3.96, 95%CI 1.56-10.05, p=0.004). The RAD51 test was able to significantly discriminate tumors sensitive to carboplatin (interaction test, p=0.02) [45]. This benefit maintained statistical significance also in the multivariate

analysis after adjustment for predefined clinical-pathological variables (OR=7.52, 95%CI 2.21-25.61, p=0.001) [45]. In terms of DFS, the benefit of adding carboplatin was similar in RAD51-high (HR=0.40, 95%CI 0.12-1.29, log-rank p=0.11) and RAD51-low (HR=0.45, 95%CI 0.16-1.25, log-rank p=0.11) groups[45]. Regarding OS, no statistically significant association was found from the addition of carboplatin in RAD51-high (HR=0.34, 95%CI 0.09-1.26, log-rank p=0.09 and RAD51-low (HR=0.82, 95%CI 0.23-2.90, log-rank p=0.76) tumors[45].

The RAD51 assay was also performed on samples from early TNBC patients enrolled in PETREMAC trial and treated with PARPi Olaparib in neoadjuvant setting[18]. Functional HRD, as defined by low RAD51 scores, correlated to HR mutations/BRCA1 methylation status, as well as olaparib response[18].

1.6. HRR pathway and immune system activation in BC[46]

HRD and the innate immune response: STING and RIG pathway

Several preclinical and clinical data suggested the importance of the innate immune system in the response to HRR-deficient tumors. Remarkably, an emerging role appears to be played by the stimulator of interferon genes (STING) pathway, primarily known as an innate immune pathway involved in the response to viral infections[47]. Elevated levels of basal DNA damage results in the increase of cytosolic DNA (cDNA) which induces an activation of cGAS and, consequently, the translocation of STING from the endoplasmic reticulum to the nucleus (**Figure 3**)[48]. There, STING leads to the transcription of several IFN type I -related genes by IRF3 activation, [48] thus inducing the production of IFN type I and chemo-attractive cytokines, i.e. CXCL10 and chemokine (C-C motif) ligand 5 (CCL5). NK cells, M1-like macrophages and both T and B-lymphocytes are recruited in an Ag-independent manner (**Figure 3**)[48]. Nonetheless, high levels of DNA damage also activate the so called “alternative STING pathway” by ATM-TRAF6, inducing the production of IL-6 and TGF-β

thus leading to the recruitment of pro-tumor M2-like macrophages and regulatory T cells (Tregs)[48]. Furthermore, ATM-TRAF6 activates the transcription factor Nuclear Factor kB (NFkB) and induces the upregulation of PD-L1 (by tumor cells) that may elicit immune-evasion (**Figure 4**)[47]. Besides this mechanism, the IFN type I itself (secreted upon STING activation) is the main factor inducing transcription and expression of PD-L1. We and others recently showed that treatment with PARPi and platinum chemotherapy increases DNA damage and, consequently, enhances the STING pathway activation, inducing the recruitment of immune cells[47, 49, 50]. In addition, the activation of the "alternative STING pathway" with the upregulation of PD-L1 pave the basis for promising combinations with immune-checkpoints inhibitors targeting the PD-1 pathway[47, 50].

Prognostic and predictive role of Tumor Infiltrating Lymphocytes (TIL) in BC

Despite having traditionally being considered non-immunogenic, a certain number of studies revealed that BC can be characterized by a high expression of immune gene signatures and a high extent of TIL. This is particularly true for TNBC and HER2-positive subtypes (reviewed in [51]). Notably, high TIL extent is associated with improved survival and with better responses to standard treatments (reviewed in [51–53]). So far, a variety of trials have been performed and is ongoing to evaluate the effects of ICB, particularly in TNBC (reviewed in [54]). Recently the anti-PD-L1 atezolizumab, has been approved as the first immunotherapeutic agent for the treatment of metastatic TNBC patients in the 1st line setting, in association with chemotherapy (nab-paclitaxel), following the impressive results obtained in the IMpassion 130 trial[55]. This study demonstrated that atezolizumab plus nab-paclitaxel prolonged progression-free survival (PFS) in the entire TNBC group and in the PD-L1-positive subgroup. The treatment with this agent was safe. However, to improve the efficacy of immunotherapy in BC, it is mandatory to better define the ideal candidates to these expensive and potentially toxic treatments. One of the best predictors of benefit were stromal TIL assessed on H&E

tissue sections ([56–58]) and $CD8^+$ TIL by IHC[57]. Remarkably, efforts are being performed in order to standardize TIL scoring on H&E tissue slides, not only in BC (both primary tumors and residual disease) [59, 60] but also in other solid tumors and in metastases in order to render this biomarker more reproducibly assessable by pathologists[19, 20].

HRD and adaptive immunity in breast cancer: TMB and TIL

It is thought that pathogenic gBRCA1/2 mutations could increase the likelihood of immunogenic somatic mutations (neo-Ags), which are generated for the essential role played by BRCA1/2 in repairing DSBs[63]. Although BC has a relatively low number of non-synonymous mutations compared to melanoma and non-small cell lung cancer [64], a study of 560 breast tumor genomes found numerous somatic mutations [65] particularly in 90 tumors with alterations in BRCA1/2 genes. Further, the presence of gBRCA1 mutations was associated with TP53 mutations and a high sensitivity to DNA cross-linking agents[66].

A pooled analysis of five clinical trials, including patients with TNBC undergoing neoadjuvant platinum-based treatment, was conducted to evaluate the association between TIL, HRD status and somatic BRCA1/2 mutational status[19]. TIL and HRD status were independent and non-overlapping predictors of benefit from neoadjuvant chemotherapy. Noteworthy, there were no differences in the extent of stromal TIL and intratumoral TIL between HRR-deficient and HRR-proficient tumors and a similar observation was detected between somatic BRCA1/2 mutational status and HRD binary score[19]. Moreover, in the GeparSixto trial, Lymphocyte Predominant Breast Cancers (LPBCs), namely tumors with a TIL infiltration higher than 60% of sTIL or itTIL were equally distributed between HRR-deficient and proficient samples [7]. These results are in line with data from a retrospective study by Solinas et al [67], showing that the extent of TIL, TLS, the expression of PD-1 and PD-L1 is similar between gBRCA1/2-mutated and WT high-risk TNBC. However, a remarkable

difference was the smaller number of TIL^{neg} tumors (<10% stTIL) in the gBRCA1/2-mutated group, suggesting these tumors may have a higher TIL set point than their WT counterparts in this special TNBC cohort of patients that underwent a genetic counselling for their personal or familial history of BC or ovarian cancer. The significant increase in TIL^{pos} tumors observed in the gBRCA1/2-mutated group supports this view[68].

Indeed, in a recent study where somatic aberrations, TME characteristic, and survival of tumors from different origins were considered, highly mutated BRCA1/2 tumors clustered in the IFN-γ dominant (C2) immune subtype [69]. This phenotype was characterized by: a better prognosis; the highest extent of the lymphocytic infiltrate, a $CD8^+$ T cell associated signature; the highest M1-like macrophage content; the highest proliferation signature; the lowest TAMs/lymphocyte ratio; the lowest Th1/Th2 ratio; the highest M1/M2-like macrophages polarization; the greatest T cell receptor (TCR) diversity. These tumors are thought to be edited, signifying that they underwent changes in the immunogenicity due to the immune response, resulting in the emergence of immune-resistant variants[70].

1.7. Hypothesis

As future perspectives, research is needed to confirm if RAD51 assay might be useful to identify BC and HGSOC patients who may benefit from PARPi beyond gBRCA1/2 mutations and platinum-sensitivity. Also, the prognostic role of HRD should be further investigated with ad hoc trials in order to recognize patients with early BC candidates for a targeted strategy. Prospective comparison between HRD-genomic scars and functional dynamic tests such as the RAD51 assay is encouraged. During my PhD program, we answered to these research questions by: 1) validating the RAD51 assay as a predictive biomarker of response to PARPi, independently of gBRCA1/2 status, in pre-clinical samples; 2) testing the RAD51 assay on early TNBC patients administered with platinum-

free neoadjuvant chemotherapy; 3) comparing the RAD51 assay with genomic HRD assays on HGSOC samples.

2. Methods

2.1. In vivo experiments on PDX models (in collaboration with Vall d'Hebron Institute of Oncology)

Generation of PDX models and in vivo treatment experiments

Fresh tumor samples from patients with HRR-related breast (triple negative, luminal B or HER2-positive), ovarian or pancreatic cancer were collected for diagnostic and for implantation into nude mice under an institutional review board (IRB)-approved protocol. The human biological samples were sourced ethically and their research use was in accord with the terms of the informed consents under an IRB/EC approved protocol. Experiments were approved by the Ethical Committee of Animal Experimentation of the Vall d'Hebron Research Institute. All animal studies were ethically reviewed and carried out in accordance with European Directive 2010/63/EEC and the GSK Policy on the Care, Welfare and Treatment of Animals. The PARPi response criteria was based on the percentage of tumor volume change. Responders included models that exhibited Complete Response (CR), Partial Response (PR) and Stable Disease (SD) and Non-Responders included Progressive Disease (PD).

DNA sequencing and genomic HRD by scars or signatures

DNA was extracted from PDX samples using DNeasy Blood & Tissue Kit (Qiagen). Three genomic scar/signature assays were performed: the Myriad's myChoice HRD test carried out at Myriad Genetics on DNA extracted from a subset of Xentech's PDX (using NucleoBond AXG100 kit, Macherey- Nagel), HRDetect and the Genomic Instability Score (GIS: levels of allelic imbalance, loss off heterozygosity, number of large-scale transitions) performed at Wellcome Trust Sanger Institute on DNA extracted from a subset of VHIO's PDX as described in[71] and[72], respectively.

BRCA1 promoter hypermethylation

BRCA1 promoter methylation was measured using methylation-specific multiplex ligation-dependent probe amplification (MS-MLPA; MRC Holland, Amsterdam, the Netherlands) according to manufacturer's instructions. Two of the xenografts generated in CRUK/UCAM (STG139 and STG201) had been previously tested using reduced-representation bisulfite sequencing (RRBS)[73] and further validated using MS-MLPA. Positive controls of BRCA1 promoter hypermethylation were used (T127 and/162).[74]

BRCA1 mRNA expression

RNA was extracted from PDX samples (15–30 mg) by using the PerfectPure RNA Tissue kit (five Prime). The purity and integrity were assessed by the Agilent 2100 Bioanalyzer system, and RNA-seq was performed in Illumina HiSeq 4000 (Illumina). Log2 transformation was used for data analysis.

Immunofluorescence staining and scoring

The following primary antibodies were used for immunofluorescence: rabbit anti-RAD51 (Abcam ab133534, 1:1000), mouse anti-geminin (NovoCastra NCL-L, 1:100 in PDX samples, 1:60 in patient samples), rabbit anti-geminin (ProteinTech 10802-1-AP, 1:400), mouse anti-BRCA1 (Santa Cruz Biotechnology sc-6954, 1:50), mouse anti-BRCA1 (Abcam ab16780, 1:200), mouse anti-phospho-H2AX (Millipore #05-636, 1:200). Goat anti-rabbit Alexa fluor 568 (Invitrogen; 1:500), goat anti-mouse Alexa fluor 488 (Invitrogen; 1:500), donkey anti-mouse Alexa fluor 568 (Invitrogen; 1:500), and goat anti-rabbit Alexa fluor 488 (Invitrogen; 1:500) were used as secondary antibodies. The immunofluorescence was performed as described in [26].

Biomarkers were quantified on FFPE PDX, PDC or patient tumor samples by scoring the percentage of geminin-positive cells with 5 or more nuclear foci of any size[26]. Geminin is a master regulator of cell-cycle progression that enables to mark for S/G2-cell cycle phase.[75] Scoring was performed onto

life images using a 60x-immersion oil lens. One hundred geminin-positive cells from at least three representative areas of each sample were analyzed. Samples with low □H2AX (< 25% of geminin-positive cells with □H2AX foci) or with < 40 geminin-positive cells were not included in the analyses, due to insufficient endogenous DNA damage or tumor cells in the S/G2-phase of the cell cycle, respectively. The mouse anti-geminin antibodies used in this study are human-specific so that they did not cross-react with mouse stroma.

PDC ex vivo cultures

Patient-derived tumor cells (PDC) were isolated from 24 PDX through combination of mechanic disruption and enzymatic disaggregation following a previously described protocol.[73] Briefly, PDX tumors not bigger that 500 mm^3 were freshly collected in DMEM/F12/HEPES (GIBCO) after surgery resection, minced using sterile scalpels and dissociated for a maximum of 90 minutes in DMEM/F12/HEPES (GIBCO), 1 mg/ml collagenase (Roche), 100 u/ml hyaluronidase (Sigma-Aldrich), 5% BSA (Sigma-Aldrich), 5 µg/ml insulin and 50 µg/ml gentamycin (GIBCO). This was followed by further dissociation using 0.05% trypsin (GIBCO),1 u/ml dispase (StemCell technologies) and 1 mg/ml DNase (Sigma-Aldrich). Red blood cell lysis was done by washing the cell pellet with 1X Red Blood Cell (RBC) Lysis Buffer containing ammonium chloride (Invitrogene). Then, cells were resuspended RPMI 1640 with GlutaMAX medium (Gibco) supplemented with 2% of heat inactivated fetal bovine serum (Gibco), 1 ul/ml ROC inhibitor, 20 ul/ml B27, 0.02 ul/ml EFG, 0.2 ul/ml FGF10, 0.2 ul/ml FGF2. To obtain FFPE blocks from PDC cultures, cells were seeded at 2x105 cells/ml in 6-well plates (BD Biosciences). After 24 hours, PDC were treated with vehicle (DMSO) or 2.5 µM olaparib and incubated at 37ºC in 5% of CO_2. Vehicle and olaparib-treated cells were recovered after 48 hours and centrifuged at 2000 rpm for 1 minute to obtain a cell pellets which were washed twice with PBS. Pellets were fixed in 4% paraformaldehyde (PFA) overnight at 4ºC and PFA

was replaced by 70% ethanol the following day. Then, pellets were centrifuged at 2000 rpm for 10 minutes and the supernatant was discarded. Finally, pellets were extracted using a needle, introduced in cassettes and maintained in 70% ethanol until embedded in paraffin.

For half maximal inhibitory concentration (IC50) analysis, cells (2 x 10^3 cells/well) were seeded into 96-well plates (BD Bioscience) and were treated the following day with different concentrations of olaparib for 14 days. The treatments and media were refreshed every 2 days. Olaparib-sensitive and -resistant PDX were included in every batch of analysis. All plates were read with CellTiter Glo® Luminiscent Cell Viability Assay (Promega) in an Infinite M200 PRO plate reader (TEKAN). Values at day 14 were subtracted with the mean background signal (no cells), normalized with values at day 0, relativized to controls (not treated cells) and plotted as the percentage inhibition against the log concentration of olaparib. IC50s values (half maximal inhibitory concentration) were calculated performing a nonlinear regression. Each experiment was repeated two times with two technical replicates.

2.2. TIL analyses on early TNBC

The pathological analysis included standard diagnostic variables and assessment of the tumor inflammatory reaction (TIL) according to current recommendations. Briefly, stromal lymphocytes were scored quantitatively on H&E stained whole-tumor slides as a continuous variable expressed as stromal percentage area within the tumor boundaries. For tumors with heterogeneous TILs, median values were calculated from multiple counts from different tumor areas. Intra-epithelial TIL were also recorded as well as tertiary lymphoid structures. Tumor regression was scored based on recommended criteria. The composition of the lymphoid infiltrate was characterized using a series of immunostain markers, as follows: LCA (clones, 2B11 e PD7/26); CD20 (L26); CD3 (2GLV6); CD4 (SP35); CD8 (SP57); CD56 (MRQ-42); CD25 (4C9); PD-1 (NAT105) and PD-L1/CD274 (SP142). Antibodies

certified for in vitro diagnostic use (CE-IVD) were purchased from Roche Diagnostic. Immunostains were performed on slides cut from FFPE specimens, processed according to standard procedure on a BenchMark (Roche) automatic immunostainer. Immunostains were developed using polymeric systems, Ultraview Detection Kit e Optiview Detection Kit (Roche).

Single markers were scored quantitatively after image digitalization as percentage stromal area, both individually and as ratios (eg.. CD8+/Foxp3+, CD20/CD3, etc). PD-L1 was evaluated on both tumor and lymphoid cells and expressed as combined score of percentage cell positivity and staining intensity.

2.3. HRD academic tests performed on HGSOC (in collaboration with Humanitas Cancer Center and Catholic University of the Sacred Heart)

LAB1

Library design

A customized capture sequencing library was designed from a modification of a commercially available kit (Agilent OneSeq Constitutional Panel, Agilent USA), spanning 12Mbp of structural genomic regions ("backbone") plus target region.

Sequencing data analysis

Pre-processing and analysis followed current best practices [https://gatk.broadinstitute.org/hc/en-us]. Briefly, samples were sequenced with NextSeq 500 (Illumina, USA). Raw FASTQ files are then aligned to the reference genome (hg19) with the BWA[76]. Variant calling was performed with VarDict[77], and ploidy and purity estimated with PureCN[78].

Somatic variant calling in BRCA1 and BRCA2 genes

Somatic variants in BRCA1/2 genes were extracted from resulting data after variant calling step, plus adjustments for purity, ploidy and allele copy number. The Cancer Genome Interpreter

(https://www.cancergenomeinterpreter.org) [Tamborero 2017] and BRCA Exchange (https://brcaexchange.org) databases were used to remove benign, likely benign, passenger (i.e. variants predicted in silico not to be tumor drivers) variants and variants of unknown significance (VUS). The complete procedure for variant calling is described in Supplementary Methods.

HRD score calculation

We calculated the HRD score using an in-house developed Python script (see Supplementary Methods), and the resulting HRD scores were then subject to a threshold (calculated as the 5th percentile from an internal data set with BRCA1/2 somatic and germline variants): HR score > 42 is meant as probable HR deficient; HR score < 42 is meant as probable HR proficient. In addition, if a sample is indicated as HR proficient but presents a mutation in BRCA1 or BRCA2, then it is considered as HR deficient; if a sample is indicated as HR proficient and has no other mutations, then it is considered as HR proficient.

LAB2

Library preparation for shallow whole genome sequencing (sWGS)

DNA libraries for Illumina sequencing were prepared by using the KAPA HyperPlus kit (Roche Sequencing Solutions, Pleasanton, CA, US). The library preparation was performed using a concentration of extracted DNA to 50 ng/µl according to the manufacturer's protocol except for the following modified steps: to achieve an average DNA fragment size between 180 – 220 bp we performed an enzymatic fragmentation for 30 minutes at 37 °C; the ligation reaction was incubated at 20 °C for 1 hour. Finally, the quality and integrity of libraries were assessed on the TapeStation (Agilent Technologies, Santa Clara, CA, USA). The concentration of all libraries was measured using Qubit dsDNA HS (High Sensitivity) assay kit on Qubit® Fluorometer 4.0 (Invitrogen Co., Life Sciences, Carlsbad, USA), after an equimolar pool was prepared. The sequencing reaction was carried

out on the Illumina NextSeq550 Dx System (Illumina, San Diego, CA, USA), loading the pool with a concentration of 1.2 pM and 2% Phix 1,5 pM.

Sequencing data analysis

Overall statistics for each NGS run were evaluated with the latest available version of the Illumina Run Manager software installed on the instrument. Two different NextSeq500/550 Mid output kit (300 cycles) were loaded on NextSeq550 Dx in RUO mode to sequence the training set (n=24 samples). Eight samples were analyzed in the first run and 16 samples in the second, including 5 analytical duplicates from the previous one. The test set (n=100) was divided in two groups of 50 samples without duplicates on two independent NextSeq500/550 High output kit (300 cycles).

For each run quality of the sequenced samples was checked using MulitQC software. Fastq files were then aligned to the hg19 reference genome using BWA-MEM. Moreover, supplementary and duplicate reads were removed from the BAM files using Samtools and PicardTools' MarkDuplicates, respectively. At this stage, an overall view of the sequencing alignment data was performed to detect biases in the sequencing and/or mapping of the data. To check the aligned BAM files, we used 'Multi Sample BAM QC' option available in the platform-independent tool Qualimap v2.2.1. All the BAM files that have met quality criteria, were sent to downstream analysis. To estimate chromosomal aberrations in our samples we used the DNAseq R package so that sequencing genome data are divided into non-overlapping fixed-sized bins, then the number of reads in each bin counted and corrected for sequence mappability and GC content. Finally reads were filtered to remove spurious regions in the genome.

HRD score calculation

HRD scores were calculated for each samples using whole genome sequencing data at low coverage (0.4-0.8X) using 6 different integrated models encompassing variable sliding windows spanning 5 to

1000 Kbases. The HRD score was then estimated by measuring the level of agreement in the segmentation profiles of each sample and was independently calculated without considering the BRCA status.

BRCA testing

To investigate the BRCA and non BRCA gene status (HRR assessment) of our tumor samples, we used the TruSight™ Tumor 170 kit (namely TS170 - Illumina, San Diego, CA, USA), an enrichment-based targeted panel. This next-generation sequencing (NGS) assay is designed to cover a wide range of genes and variant types associated with solid tumors targeting DNA variants from formalin-fixed, paraffin-embedded (FFPE) tumor samples. NGS sequencing was performed following the manufacturer's instructions on 88 out of the 100 somatic samples previously analyzed for HRD, since the remaining 12 out of 100 did not meet the quality criteria for this assay.

Specifically, the libraries for TS170 were prepared using 50 ng of gDNA performing the steps as follows. gDNA was fragmented to about 250 bp size using the Covaris M220 Focused-ultrasonicator and microTUBE-50 AFA Fiber Screw-Cap (Covaris, Woburn, MA) with the following settings: peak incident power 75 watts, duty factor 15%, 1000 cycles per burst, 360 seconds treatment time, 20° c temperature.

According to the TS170 protocol, the regions of interest are hybridized to biotinylated probes, magnetically pulled down with streptavidin-coated beads, and eluted to enrich the library pool. Finally, the libraries are normalized using a simple bead-based protocol before pooling and sequencing. The sequencing reaction was carried out on the Illumina NextSeq550 Dx System (Illumina), loading the pool with a concentration of 1.8 pM and 2% Phix 1,5 pM using a High Output flow cell kit (Illumina).

DRY lab

The analysis on 88 high grade serum carcinoma was performed with the Clinical Genomic Workspace (CGW) Pierian DX IVD pipeline with default settings for IV diagnostics.

The software classifies all the variants as per the AMP classification system into tiers IA, IB, IIC, IID, III and IV. These tiers are stratified by clinical utility ('actionability' for clinical decision-making as to diagnosis, prognosis, treatment options, and carrier status) and previously reported data in the medical literature. Variations found in gnomAD (https://gnomad.broadinstitute.org/) that have ≥1% minor allele frequency (except those that are also in Clinvar denoted as clinically relevant, used in a clinical diagnostic assay, or reported as a mutation in a publication) are classified as known polymorphisms. Moreover, all DNA variants (SNVs, Insertions, Deletions, MNVs, and CNVs) are included only if the minimum variant allele frequency is higher than 5% and if they had a coverage depth of ≥ 100x (SNVs) and ≥ 250x (insertions, deletions and MNVs) to reliably call small DNA variants (SNVs, insertions, deletions and MNVs).

2.4. Statistical analysis

In vivo experiments and early BC

Data were analyzed with GraphPad Prism version 7.0 software (GraphPad, La Jolla, CA). Bars represent the median of at least two technical replicates, unless otherwise stated. Shapiro–Wilk test was used to assess normality of data distributions. If the null hypothesis of normal distribution was not rejected, statistical tests were performed using paired and unpaired two-tailed t-test (for two groups comparison of PDC and/or patient samples, and HRD score by Myriad in PDX). Otherwise, the non-parametric Mann-Whitney or Wilcoxon signed-rank test was used (for two groups comparison of RAD51/geminin and HRDetect score in PDX). The receiver operating characteristic (ROC) curve and the area under the curve (AUC) were calculated to estimate the prediction capacity of Myriad's myChoice HRD test and RAD51 scores to PARPi response. For AUC comparison, a two-sided

bootstrap test was used by means of statistical package *pROC* in R software. Additionally, sensitivity, specificity, positive (PPV), and negative (NPV) predictive values were calculated using the pre-established cut-off. Cohen's kappa coefficient was calculated to estimate the agreement of RAD51 status between PDX and patient's sample. To calculate the association between RAD51 score in PDX and in PDC, and between RAD51 in PDX and patient samples, a linear regression model was fitted to estimate the R-squared with CI 95%.

High Grade Serious Ovarian Cancer

Baseline characteristics of patients were described using median and interquartile range for continuous variables and frequencies and percentage for qualitative variables.

To evaluate the concordance of HRD academic tests with the commercial Myriad myChoice, it was calculated that a sample size of 89 patients would have resulted in a two-sided 95% confidence interval (CI) with a width of 0.25 considering a Cohen's K value of 0.80 and a standard deviation of K value of 0.60. The final sample size was increased to 100 patients considering the event of inconclusive tests.

For each academic test the agreement and disagreement rate with the Myriad test were calculated. The concordance index was measured using Cohen's K statistic with 95% CI. The K statistic was interpreted as less than 0 indicating no agreement, 0.00 – 0.20 as slight, 0.21 – 0.40 as fair, 0.41 – 0.60 as moderate, 0.61 – 0.80 as substantial, and 0.81 – 1.00 as an almost perfect agreement. For BRCA status, agreement was calculated considering the number of mutations and the finding of the same mutations by the different tests.

The prognostic value of each HRR test (Myriad, LAB1, LAB2, RAD51) was investigated in terms of progression-free survival (PFS), overall survival (OS), and response rate (RR) by HRR status (HRD vs HRP).

PFS was defined as the time from registration to documented progression according to RECIST criteria, death for any cause or last follow-up date and OS was defined as the time from randomization to death for any cause or last information on vital status.

Survival curves were calculated using the Kaplan-Meier method and compared by Log-rank test. Hazard ratios (HRs) were estimated by Cox regression model. In the multivariable models the following covariates were added: age (as category <65 vs ≥65), ECOG performance status (PS) (0 vs 1-2), Residual disease (None; ≤1cm; >1cm/not operated), FIGO stage (III vs IV).

The response rate by RECIST 1.1 investigator assessed was defined as the proportion of patients who had a complete response or partial response. Exact confidence interval of proportion of respondent patients was calculated with Clopper-Pearson method.

All the analyses were performed with STATA 14 MP (StataCorp. 2015. Stata Statistical Software: Release 14. College Station, TX: StataCorp LP.)

2.5. Sample size

In vivo experiments

The main goal was to analyze in a cohort of PDX models whether the accuracy to predict response to PARPi was different using mutations in HRR genes, genomic HRD tests or the RAD51 assay. Our PDX panel was enriched with models having HRD, as >50% of models derived from patients with a germline HRR gene alteration. In addition, it was expected to find >70% of HRD-positive tumors by genomic scars since the vast majority of the PDX tumors are TNBCs according to immunohistochemistry characterization of estrogen and progesterone receptor and the Her2 status.[5] The accuracy to predict PARPi response using HRR-gene mutations was expected to be 70% while the accuracy of RAD51 assay was estimated to be 92%.[16, 43] In order to detect such a difference using a 1/2.5 ratio with at least 90% power and two-sided type I error of 0.05, at least 41 PDX samples

with HRR-gene mutations and 103 PDX samples with RAD51 assay information were required. Sample size calculation was based on exact binominal distribution. Assuming that not all HRR-gene tests and RAD51 assays would provide informative results, an attrition rate of 5% was estimated, and consequently, a total of 109 PDX samples were needed.

Early BC patients

148 high-risk BC patients, namely histologically confirmed TNBC or early onset BC (≤ 35 years old) or gBRCA1/2-mutated BC were tested for RAD51 assay and TIL extent. Patients were admitted at 6 Italian Hospitals of the "Gruppo Oncologico Italiano di Ricerca Clinica" (GOIRC), and treated with (neo)adjuvant chemotherapy based on anthracyclines, taxanes and cyclophosphamide.

High grade serious ovarian cancer patients

From the whole population of the MITO16A/MaNGO-OV2 trial, we randomly selected 100 patients with high-grade serous and endometrioid cancer and enough material to allow all the assays done on the same specimen. In order to evaluate the representativeness of the enrolled population for the overall MITO16A/MaNGO-OV2 trial population, the characteristics of the identified patients were compared with those of the overall population of the MITO16A/MaNGO-OV2 trial, in terms of age, ECOG performance status (PS), residual disease and FIGO stage; PFS and OS in the two populations were also described. Details of the MITO16A/MaNGO-OV2 trial have been reported by Daniele et al[79]. In brief, the main enrolment criteria were as follows: FIGO stage IIIB-IV, previously untreated epithelial ovarian cancer, ECOG PS 0–2, adequate organ function and no prior major systemic disease. All patients in the MITO16A/MaNGO-OV2 trial received carboplatin and paclitaxel plus bevacizumab, followed by bevacizumab monotherapy, up to a maximum of 22 total cycles.

3. Results

3.1. In vivo validation

PARPi antitumor activity in a series of PDX

One hundred and nine patient-derived models from three *BRCA*-associated cancers were established, namely from breast, ovarian and pancreatic cancers, both from primary and metastatic tumors (**Figure 5; Table S1**)[25, 26]. The antitumor activity of the PARPi olaparib or niraparib was assessed in 96 PDX models derived from 65 TNBC, 24 hormone receptor-positive (HR+) BC, 1 HER2-positive (HER2+) BC, 4 HGSOC and 2 PaC patients (**Table S1**). Upon PARPi treatment *in vivo*, the best response according to modified RECIST criteria was: complete response (CR) in 12, partial response (PR) in 10 and stable disease (SD) in 7 PDX models, totaling 29/109 sensitive models. Sixty-seven PDX models were PARPi-resistant (PD, progressive disease, as best response) (**Figure 6A**). Additional 13 resistant models were generated from nine PARPi-sensitive PDX after prolonged exposure and steep progression to olaparib. Time to progression was not observed to be associated with the type of HRR alteration. In total, 80/109 models were resistant to PARPi.

Identification of HRR alterations in PDX and association with PARPi response

Forty out of 96 (42%) PDX models did not present alterations in HRR genes and did not respond to PARPi treatment (**Figure 6A,B**). The remaining 56 models harbored alterations in HRR genes and presented differential responses to PARPi (**Figure 6A,B**). Pathogenic biallelic variants in BRCA1 were identified in 25 models (9 sensitive and 16 resistant) and BRCA2 pathogenic biallelic variants were detected in 13 models (10 sensitive and 3 resistant). BRCA1 epigenetic silencing, evaluated by lack of BRCA1 transcript by RNA-sequencing (cut-off □1 tmp) and lack of functional BRCA1 nuclear foci by immunofluorescence (IF; cut-off □10%) was found in 13 PDX (6 sensitive and 7 resistant). We identified biallelic frameshift mutations in *PALB2* in three PARPi-sensitive models (PDX093, T298, ST897) and homozygous loss of the gene encoding the RAD51 paralog *XRCC3* in a PARPi-sensitive PDX (HBCx14, labelled as “other HRR genes” in **Figure 6A,B; Table S1**). Taken together,

our analyses identified that all the PARPi-responsive PDX models in the cohort had at least one alteration in the HRR genes BRCA1, BRCA2, PALB2 or XRCC3.

Whole Exome Sequencing (WES) also revealed mutations that could explain mechanisms of resistance to PARPi in HRR-altered PDX (**Figure 6C**). Three models (PDX093OR6, PDX332 and PDX405OR100) harbored mutations in PALB2 or BRCA2 that were compatible with HRR gene reversions. Three additional BRCA1-mutant models presented alterations in the 53BP1-shieldin pathway, which have been shown to confer PARPi resistance (HBCx28, PDX127, PDX230OR1) (**Table S1**).[80–82] Interestingly, BRCA1 nuclear foci (cut-off >10%) were detected in 7 out of 25 BRCA1-mutant models, underscoring the high prevalence of re-expression of BRCA1 proteins lacking relevant domains in this panel, which is considered hypomorphic (**Table S1**). The presence of BRCA1 proteins lacking relevant domains in tumors with mutations in the RING, exon 11 or the BRCT domains of BRCA1 has been associated with resistance to PARPi (**Figure 6C**; **Table S1**).[83–85] In addition, BRCA1 nuclear foci were detected in 4 out of 11 BRCA1 low models upon acquisition of PARPi-resistance. Finally, three models (PDX124OR, PDX377OR1 and PDX377OR2) were PARPi-resistant without substantial of HRR restoration, according to their levels of BRCA1 and RAD51 nuclear foci when compared to their sensitive counterparts (PDX124 and PDX377) ("RAD51-independent" in **Figure 6C**). Altogether, our genomics, transcriptomics and BRCA1 protein foci analyses identified likely mechanisms of PARPi resistance in half of the HRR-altered, non-responsive models.

We calculated the sensitivity, specificity, positive predictive value (PPV) and negative predictive value (NPV) for PARPi response of HRR gene mutations or low BRCA1 expression (mRNA or nuclear foci, **Table 3**). These two HRD biomarkers showed similar accuracy (67% and 69%,

respectively). In summary, our data confirmed that genetic and epigenetic alterations in HRR genes had limited accuracy predicting PARPi sensitivity.

Quantification of genomic HRD in PDX and association with PARPi response

We evaluated the association between the genomic scar Myriad myChoice® HRD and PARPi response. Genomic HRD was quantified in a subset of 41 PDX models, 11 of which harbored a mutation in BRCA1/2 or *PALB2*. All the HRR-gene mutated samples were HRD-positive (cut-off≥42) (**Table S1**). In addition, the test identified as HRD-positive nine tumors lacking BRCA1 expression (BRCA1 low) of which two were known to previously harbor BRCA1 promoter hypermethylation (named as "WT with history of HRD")[86]. All PARPi-sensitive PDX were HRD positive and the median of HRD values was higher in PARPi sensitive than in PARPi resistant models (**Figure 7A**, median of 67 vs 36, p=0.0002). Nonetheless, 12 out of 29 PARPi-resistant PDX were also HRD positive. Accordingly, the genomic HRD test showed a limited accuracy for predicting PARPi responses (71%), similar to HRR-gene mutations or assessment of BRCA1 mRNA expression or BRCA1 nuclear foci (**Table 3**).

We also quantified the whole genome sequencing (WGS)-derived HRD signature named HRDetect in an independent subset of 15 PDX, 10 of which were derived from BRCA1/2 mutation carriers and 11 from metastatic biopsies (**Table S1**). All PDX derived from patients with BRCA1/2-associated BCs had high HRDetect values (cut-off>0.7[71]). The GIS score in these models was concordant with HRDetect. As observed for the Myriad myChoice® HRD scores, all PARPi-sensitive tumors had high HRDetect values, but 8 out of 11 PARPi-resistant tumors also had high HRDetect values. In summary, these data show that genomic HRD tests provide very high sensitivity and NPV but limited specificity and PPV to predict PARPi response.

Association of functional HRD by RAD51 and PARPi sensitivity

We further aimed to investigate the functional HRD status of this PDX cohort, scoring the percentage of tumor cells with RAD51 nuclear foci in the S/G2-phase of the cell cycle (geminin-positive).[25, 26] When comparing RAD51 with HRR-gene alterations, we noted that HRR-altered models had significantly lower levels of RAD51 values than HRR-WT PDX (median of 16% vs 50%, $p<0.0001$), albeit 61% of HRR-gene altered tumors had high RAD51 scores. Similarly, 54% of tumors identified as positive for genomic HRD presented high RAD51 scores (**Figure 7B**).

Next, we explored the potential of the RAD51 score to predict PARPi response. PARPi-sensitive models showed a significantly lower percentage of RAD51-positive cells than the PARPi-resistant ones (median of 1% vs 38% respectively, $p<0.0001$; **Figure 7C**). Moreover, we observed an increase of the RAD51 score in the 13 models of acquired PARPi resistance derived in laboratory conditions, compared to their sensitive counterparts (median of 33% vs 1%, $p=0.0006$). This result highlights the dynamic nature of the RAD51 test.

Using the pre-established cut-off for RAD51 (RAD51≤10%),[23] the RAD51 assay demonstrated high sensitivity (90%) and specificity (98%), along with well-balanced PPV (93%) vs NPV (96%) (**Table 3**). The RAD51 test predicted PARPi response in PDX harboring BRCA1, BRCA2 and PALB2 mutations (accuracy 92%) and in PDX without mutation in these genes (accuracy 98%). The accuracy of RAD51 to predict PARPi response was significantly higher than the obtained with the genomic HRD test (95% vs 71%, $p<0.001$). Of note, the discordant models exhibited an intermediate response to PARPi. A comparative receiver operating characteristic (ROC) analysis was conducted for RAD51 scores and Myriad myChoice® HRD test in a subset of 41 samples and revealed that the ROC AUC for the RAD51 assay was superior than for the genomic HRD score (0.97 vs. 0.81, $p=0.03$; **Figure 7D**). Altogether, these data validate the pre-established RAD51 assay score cut-off and demonstrate

that assessment of RAD51 nuclear foci by immunofluorescence is the most accurate and dynamic HRD biomarker for predicting PARPi response (**Table 3**).

Platinum response as biomarker of PARPi sensitivity

We established cisplatin response in a subset of 56 PDX, of which 51 were derived from breast cancers (**Figure 8A**). While most of the PARPi-sensitive models were also sensitive to platinum (18/21, 86%), none of the PARPi-resistant PDX restoring BRCA1 function were platinum sensitive (0/8, 0%). As expected the two 53BP1-dependent, PARPi-resistant PDX were platinum sensitive (2/2, 100%).[87] We observed that platinum response provided lower accuracy to predict PARPi response than the RAD51 score (54% vs. 95%, **Table 3**). Regarding RAD51 scores and cisplatin response, we observed that cisplatin-sensitive PDX models had overall lower values of RAD51 than cisplatin-resistant PDX (median of 12% vs 21%, p=0.02, **Figure 8B**). However, 16/31 of the cisplatin-sensitive models presented high RAD51 scores, which suggests that these models carry deficiencies in other DNA repair pathways involved in repair of platinum-induced damage (e.g. nucleotide excision repair or Fanconi anemia pathway). Accuracy of the RAD51 assay to predict cisplatin response was similar to HRR-gene mutations or to BRCA1 epigenetic silencing (64%, 61% and 63%, respectively; **Table 4**). These results suggest that the RAD51 assay could help to identify patients who are likely to respond to platinum-based treatments with a similar accuracy of other HRD tests currently used in clinical practice.

Patient-derived models recapitulate patient's HRD status and in vivo response to PARPi

RAD51 status in PDX were highly concordant with the corresponding patient's FFPE tumor sample that was taken at the same time-point when the patient-derived xenograft model was established (Cohen's kappa=0.93, **Figure 9A**). In agreement, the PDX response to PARPi or platinum was also

highly concordant to the patient's response to the respective drug (30 out of 36, 83% concordance, **Table S2**).

Patient-derived tumor organoids from HGSOC are being established to assess drug responses to targeted drugs in a real-time manner.[88] Therefore, we further assessed the ability of patient-derived tumor cells (PDC) to recapitulate the HRD status of the PDX and the *in vivo* responses to PARPi. In a cohort of 14 models, the RAD51 score in PDC was highly concordant with the score in PDX, both when the models were PARPi-treated (kappa coefficient=0.68) or left untreated (kappa coefficient=0.74, **Figures 9B**). Concordantly, treatment with olaparib resulted in lower half maximal inhibitory concentration (IC50) values in 24 PDC derived from PARPi-sensitive PDX than from resistant ones (10^{2}nM vs $10^{2.9}$nM, p=0.017, **Figures 9C,D**). In summary, we demonstrated that both PDX and PDC recapitulate patient's HRD status and *in vivo* response to PARPi.

3.2. Immune-environment characterization in PDX models

In PDX models, PD-L1 was equally expressed in sensitive and resistant untreated samples by RNAseq and RPPA. We performed PDL1 staining by IHC in 26 PDXs samples: in non-responders there was a marked increase in PD-L1 expression except for PDX196, 127 and JAL71OR that harbour ATM/ATR pathway alterations [89], PDX270 that harbours a mutation in CD274 and PDX339 that have low PD-L1 expression by RNAseq (**Figure 10**). We compared PD-L1 expression between the correspondent patient and PDX and PDC in a small cohort of model and it was quite similar.

cGAS expression was not induced upon PARPi treatment in most of the sensitive model. According to Ghosh et al[90], this could probably due to the fact that cGAS often presents epigenetic alterations which are not solved upon PARPi.

Interesting, 12 out of 20 non-responding models (SD+PD) harbor mutations in STING pathway genes (i.e. IFNA10C20* mutation and IFIT2 amplification in 5 and 3 resistant PDXs, respectively).

HLA ABC expression increases in all sensitive models upon PARP inhibition.

We performed CD45 staining (leucocytes) by IHC in 27 PDX samples: intratumoral CD45+ cells statistically significantly increased after olaparib treatment, in particular in the responding samples (p=0.03). Interestingly, peritumoral CD45+ cells increased after olaparib treatment in resistant tumors (**Figure 11**). We performed the CD56 staining (NK cells) by IHC in 27 PDXs samples: peritumoral NK cells increase after olaparib treatment, no significant modification was observed at stromal and intratumoral levels. We performed the CD11b staining (myeloid cells) by IHC in 27 PDXs samples and in most of the sensitive cases, CD11b+ stromal cells increased after olaparib treatment (p=0.08), while decreased or slightly increased in the resistant models. CD45 positive cells were not mainly NK cells or myeloid cells, according to their IHC profile.

To better understand the role of the immune system in PARPi response, we performed a differential expression analysis between resistant and sensitive samples by RnaSeq and, based on these data, olaparib resistant PDX seemed to have a negative regulation of leucocyte proliferation (**Figure 12**). Several pro-inflammatory genes (TNF, ILA1a, IL33, CXCL11) are statistically significant more expressed in the resistant untreated PDX samples. To explore the role of the STING pathway in response to PARPi, we applied the 44-gene signature related to the STING pathway activation to our untreated PDX samples but it did not correlate with RAD51 expression nor with olaparib response.

In syngenic BRCA1-mutant mouse models, we evaluated olaparib response in vivo according to RECIST criteria and it experience a SD. We evaluated RAD51 in transgenic BRCA1 mouse and it was RAD51 negative. We performed the same IHC/IIF of PDX samples plus staining for CD3, CD4 and CD8 by IHC. Olaparib treatment in BRCA1-mutated Tg mice significantly increased infiltration of intratumoral CD3+ immune cells and stromal myeloid cells. PD-L1 (evaluated by FACS) in Tg

tumor cells was maintained upon PARPi. PD-L1 was also expressed in intratumoral CD3+ cells and increased upon PARPi.

3.3. HRD by RAD51 in early High-risk BC

Patients' characteristics

142 early High-risk BC patients were enrolled in the RADIMMUNE study: data were collected for 121 patients. Of these patients, 104 were diagnosed with TNBC, 12 were diagnosed with LumB tumor, 2 were diagnosed with LumA tumor, and 2 were diagnosed with HER2-positive tumor. Of these 121 patients, 10 have mutations in BRCA1 gene, 8 have mutations in BRCA2 gene and 2 have mutations in PALB2 gene.

19 patients were younger than 35 years old at the time of diagnosis: of these, five patients were diagnosed with BRCA1/2-mutated cancer and one patient harbors PALB2 mutation. 44 patients had lymph nodes' involvement at diagnosis. All patients were treated with neoadjuvant chemotherapy based on anthracyclines and taxanes. No patients underwent platinum-based therapy.

Of the 121 patients enrolled, 82 are still alive, 19 have died and no information was available for 20.

Of 54 patients (44.6%) who obtained pCR, 2 relapsed and one died. The median DFS of the population that obtained pCR was 60 months and the median OS was 30.2 months.

61 patients (65.4%) did not achieve pCR and, of them, 24 relapsed and 16 died. The median DFS of no pCR patients was 27 months and the median OS was 27 months. A statistically significant difference was found when comparing DFS of pCR vs no pCR patients ($p< 0.0001$) (**Figure 13**). At 5 years, pCR patients DFS was 97.6% compared to 55.8% in no pCR. Comparison of OS in the two populations also showed a statistically significant difference ($p=0.0002$) (**Figure 13**). At 5 years, the OS in pCR patients was higher than OS in no pCR patients (97.2% vs 65.04%, respectively).

HRD status in the study population

RAD51 assay was performed on 53 out of 121 patients to assess the functional HRD status, using the pre-established cut-off of a ≤ 10%. Of these, 30 patients presented a score of RAD51 ≤ 10 and were defined as HRD. HRR-altered patients presented a statistically significant lower RAD51 score compared to HRR-WT (p=0.0003, mean in the HRR-altered population=5.772 vs 20.88 in the HRR-WT with 95% CI 7.270 – 22.95) (**Figure 14**).

DFS and OS according to HRD status by RAD51

No differences in terms of DFS, according to RAD51 score, were registered (p=0.2286; HR 0.5015, 95% CI 0.1589 – 1.583) (**Figure 15**). Indeed, OS was statistically significantly higher in HRD patients compared to HRP ones (p value=0.0456; log-rank test=3.995, 95% CI 0.06861 – 1.061), with 5-year OS in the HRD population of 89.3% compared to 60.9% in the HRP (**Figure 15**).

Correlation between HRD status and pCR

No statistically significant difference was observed in terms of RAD51 score between pCR and no pCR patients (p=0.4627) (**Figure 16**). Among no pCR patients, no differences in terms of DFS were observed according to HRD status, by RAD51 (p=0.5186; 5-year DFS of 52.1% in the HRD population and 45.7% in the HRP population, HR 0.7013; 95% CI 0.2282 - 2.155) (**Figure 17**). A trend in terms of higher OS was observed in HRD patients than HRP, even no statistically significant (79.8% vs 60.2%; HR 0.5594, 95% CI 0.1934 – 1.618) (**Figure 17**).

Characteristics of immune infiltration

Immune infiltration characterization was performed in 40 out of 142 enrolled patients. Among these, 9 patients we TIL high (22%) and 29 were TIL low (73%); 2 patients were not evaluable for TIL extent (5%). When comparing TIL-High vs TIL-low patients, we observed a trend in terms of higher DFS and OS in TIL-high patients, even if not statistically significant. RAD51 score did not differ between TIL-high and TIL-low patients (p=0.2365)

Prognostic value of HRD in combination with TIL extent

We then stratified our patients according to HRD status and TIL extent in 4 subgroups: HRP/TIL-High (3), HRP/TIL-Low (7), HRD/TIL-High (5) and HRD/TIL-Low (15) patients. DFS and OS was similar among groups (p=0.3534 and p=0.0871, respectively) (**Figure 18**). Going through deeper analyses, HRD/TIL-low patients presented a trend of higher OS compared to HRP/TIL-low patients (5yOS of 88.5 % compared to 5yOS OS of 50.1%, p=0.058). In support, HRD/TIL-low tumors showed lower PD-L1 CPS compared to others (p=0.0011); no statistically significant differences were found in CD3+, CD20+, PD1+, PD-L1+ and FOXp3+ TIL neither between HRD and HRP patients nor among HRP/TIL-High, HRP/TIL-Low, HRD/TIL-High and HRD/TIL-Low patients.

3.4. Comparison between genomic and functional HRD status in HGSOC

Baseline characteristics of evaluated patients are presented in **Table 5**. Out of the 100 patients, 64 (64%) were eligible for RECIST response and 46 (72%) had complete (31, 48%) or partial (15, 23%) response. PFS was evaluated in all patients, with 80 progression events and a median PFS of 19.2 months with CI 95% (16.0 – 21.9). Median OS was 40.7 months with CI 95% (34.8 – 42.0), with 42 deaths. At multivariate analysis on PFS including age, stage, residual disease and ECOG PS, stage and residual disease were independently associated with prognosis (data not shown). **Figure 19** shows the number of patients evaluable by each test for concordance along with the reason for test failure, as detailed below.

HRR status and BRCA status assessed by the Myriad test

Out of 100 samples analyzed by Myriad, 4 (4%) samples were inconclusive for HR status because it was impossible to calculate the Genomic Instability Score; 2 (2%) samples failed for tissue quality. Consequently, Myriad HRR status was available for 94 (94%) samples, 41 (44%) of which were HR proficient (HRP), and 53 (56%) were HR deficient (HRD). BRCA1/2 status was available for 98

samples (98%) because 2 samples failed for tissue quality. A total of 66 patients out of 98 analyzed (67%) were identified with Myriad as *BRCA* wild-type and 32 (33%) as *BRCA* mutated (24 BRCA1 and 8 BRCA2-mutated).

HRR score and BRCA1/2 concordance between LAB1 assay Myriad

LAB1 HRR test was feasible in 97 out of 100 samples (97%), including 1 that failed Myriad test. With LAB1 test, 61 (63%) patients resulted deficient and 36 (37%) proficient for HRR. For 92 samples, both LAB1 and Myriad test were available. Sensitivity of LAB 1 was 98.1% (CI: 90.1% – 100%) and specificity 84.2% (CI: 68.7%– 94%). The agreement rate was equal to 0.92 (CI: 0.87 – 0.98); Cohen's K coefficient corresponded to 0.84 (CI: 0.72 – 0.96).

All 100 samples in LAB1 were tested for *BRCA*, that was mutated in 29 (29%) cases, including one case that resulted wild type at Myriad test.

Analysis of concordance of *BRCA* mutational status of Myriad and LAB1 was performed on 98 samples. Out of 32 cases mutated at Myriad test, six were wild type and one had a different mutation at LAB1 test. The agreement rate was equal to 0.92 (CI: 0.86 – 0.97); Cohen's K coefficient was equal to 0.81 (CI: 0.67 – 0.94).

HRR score and BRCA1/2 concordance between LAB2 assay and Myriad

Out of 100 samples HRR LAB2 test was feasible in 97 (97%), including 1 that failed Myriad test. With LAB2 test 56 (58 %) patients resulted deficient and 41 (42 %) proficient for HRR. For 92 samples both LAB2 and Myriad test were available. Sensitivity for LAB2 was 90.6% (CI: 79.3% – 96.9%) and specificity 84.6% (CI: 84.6% – 94.1%). The agreement rate was equal to 0.87 (CI: 0.81 – 0.94); Cohen's K coefficient corresponded to 0.74 (CI: 0.60 – 0.88). BRCA test (evaluated by the software Illumina PIERIAN) was feasible by LAB2 in 88 samples; a mutation was found in 45 (51%) cases, including 25 cases that were wild type at Myriad test. Analysis of concordance of *BRCA* mutational

status between Myriad and LAB2 was performed in 86 samples. Out of 28 cases mutated at Myriad test, 9 were wild type and four had a different mutation at LAB2 test, as evaluated by TS170 assay. In 25 out of 58 patients wild type by Myriad, a mutation was found in LAB2 test. The agreement rate was equal to 0.56 (CI: 0.44 – 0.67); Cohen's K coefficient was equal to 0.09 (CI: -0.11 – 0.30).

Concordance between RAD51 assay and HRR score by Myriad

Out of 100 samples, one case was excluded because the slides did not contain tumor cells. Ninety-nine samples were tested; ten samples did not pass the quality check due to the lack of tumor cells in the S/G2-phase of the cell cycle (< 40 geminin-positive cells); 20 samples exhibited insufficient endogenous DNA damage (< 25% of geminin-positive cells with γH2AX foci).

Thus, out of 100 samples, RAD51 assay was feasible in 69 (69%), including 2 that failed at Myriad test. According to RAD51 assay, 53 out of 69 tests (77%) were HR deficient and 16 (23%) were HR proficient. For the agreement analysis, 65 cases were available with both Myriad and RAD51 assay results. RAD51 assay had a sensitivity of 82.9% (CI: 67.9% – 92.8%) and specificity of 33.3% (CI: 15.6% – 55.3%). The agreement rate was equal to 0.65 (CI: 0.53-0.77); the Cohen's K coefficient corresponded to 0.18 (CI: -0.07 – 0.42).

Prognostic value of HRD status

Table 6 shows PFS and OS in all patients according to each test and response rate in those evaluable by RECIST. LAB2 results resulted prognostic in univariate analysis for PFS, while in the multivariate analysis Myriad, LAB1 and LAB2 were found to be correlated with PFS. RAD51 assay was not prognostic, probably due to the lower number of patients included.

Figure 20 and **21** show the curves produced by the univariate analysis for all HR test in PFS and OS, respectively.

Combined analysis of Myriad and RAD51 assay

The baseline characteristics of patients, PFS and OS according to HRR status were comparable after the Myriad test or RAD51 assay HRD/HRP stratification (data not shown).

Combining the results of Myriad and RAD 51, 34 and 6 patients were classified as HRD or HRP in both tests, respectively. Five patients were deficient to Myriad and proficient for RAD51, and 6 patients were proficient to Myriad and deficient to RAD51. These four groups are too small in number and need to be further explored prospectively. The curves are reported in **Figure 22**.

4. Discussion

In the era of precision oncology, there is an unmet medical need for optimized use of PARPi and platinum-based chemotherapy. The use of validated HRD tests in clinical practice may fill this gap. Ideally, this test should offer a fast turnaround time, be accurate and of low cost, and be close to the point of care.

In the first part of my doctoral thesis, we validated the predictive value of the RAD51-immunofluorescence test for PARPi response in a panel of patient-derived tumor models that recapitulated patients' characteristics and response to PARPi or platinum. Compared to genetic and genomic HRD tests, the RAD51 test exhibited greater PPV (93% *vs*. 43-50%), implying a better capacity to identify patients with PARPi-sensitive tumors and differentiate from those that become PARPi-resistant after restoration of functional HRR. Alike genomic HRD tests, RAD51 identified HRD in tumors with epigenetic silencing of BRCA1, as evidenced by concomitant low expression of BRCA1 mRNA expression or low BRCA1 nuclear foci. Importantly, the RAD51 test captured the dynamic nature of HRD as shown in paired models with acquired resistance to PARPi. Regarding platinum response, the RAD51 test showed similar accuracy to HRR-gene mutations (64% *vs.* 61%).

In our PDX cohort, 58% of models harbored an HRR alteration, mainly driven by genetic alterations in BRCA1/2 or epigenetic silencing of BRCA1. The preclinical response rate to PARPi amongst these models was only of 42%, highlighting the limited PPV of these selection biomarkers. We identified the

potential mechanism of resistance in half of the resistant models, encompassing the restoration of HRR-gene function in 23%, restoration of end resection mediated by the 53BP1 pathway in 4% or RAD51-independent mechanisms in 4%. RAD51-independent mechanisms of PARPi sensitivity or resistance represent a limitation for the accuracy of the RAD51 test. As an example, enhanced PARP trapping causes PARPi toxicity irrespective of HRD, such as in tumors with impaired ribonucleotide or base excision repair due to defects in RNaseH2 or XRCC1, respectively.[91, 92] Impairment of enzymes involved in other base damage repair pathways e.g., loss of ALC1 nucleosome remodeling, also confers PARPi sensitivity.[93, 94] The clinical relevance of these mechanisms is yet to be established. For 26% of the PDX in our cohort, the mechanism of resistance was not revealed by WES, but consistent with restoration of HRR by RAD51 nuclear foci formation.

The lack of PPV of the tests based on detection of HRR alterations (gene mutations or epigenetic silencing) lies upon the heterogeneity of the HRD nature. Also, even though genomic HRD tests encompass the different sources of HRD, they cannot distinguish HRR restoration. In contrast, a dynamic functional biomarker alike RAD51 can capture this heterogeneity. The discordance between genomic HRD tests and RAD51 foci is observed in half of our PDX especially in models harboring BRCA1 epigenetic silencing, likely reflecting the "soft" status of the phenotype. This observation is in line with BRCA1-low PDX exhibiting a lower time to progression with olaparib than other HRR-altered models and was pointed out in the TBCRC009 and TNT trials for platinum.[15, 44] In summary, a functional test like RAD51 foci shows an improved performance because it captures the different sources of HRD as well as its dynamic evolution.

In patients with metastatic BC, the PARPi olaparib and talazoparib have been approved for patients with a gBRCA1 or gBRCA2 pathogenic variant. Nevertheless, the overall response rate is within the range of 60%.[40, 95] In the context of a known germline condition, a functional test that measures the tumor status

of HRD before treatment initiation would likely improve patient selection for PARPi monotherapy. This would allow to optimize the prescription of effective drugs in patients who have restored HRR in their tumors. A similar scenario is expected for patients with germline pathogenic genetic alterations in PALB2 who are also sensitive to PARPi.[16, 96] In addition, efforts are also being invested in expanding the patient population who may benefit from PARPi beyond those harboring germline HRR-gene pathogenic variants with metastatic cancer. Given the positive safety profile of PARPi and the efficacy data in the early disease setting,[43, 97] PARPi have been incorporated as part of the adjuvant treatment regimens.[98] In this regard, data supporting the use of genomic HRD tests or RAD51 as predictive biomarkers of PARPi response is encouraging in early BC and analysis in larger cohorts is awaited.[17, 18]

Regarding platinum response and BC, genomic scars have failed to identify patients who may benefit both in the early and metastatic settings, and gBRCA1/2-mutations only predicted platinum response in the metastatic setting.[15, 99] Interestingly, despite cisplatin sensitivity may occur beyond HRD,[100] our preclinical data showed that the RAD51 assay may help select patients who benefit from platinum treatment, thus giving a "target" therapy option to gBRCA1/2 WT patients. In untreated TNBC, RAD51 independently predicted clinical benefit from adding carboplatin to neoadjuvant chemotherapy.[45] Further studies are needed to confirm the clinical validity of the RAD51 assay at predicting platinum response, and to verify if the test could predict response to treatments with similar mechanism of action.

Functional biomarkers of HRD are also needed for the management of HGSOC, advanced prostate cancer or pancreatic cancer. Despite quality of tumor genetic testing and interpretation of variants' effect have greatly improved in the recent years, there is still a scarcity of implementation of tumor genetic testing beyond the ovarian cancer population. Regarding platinum-sensitive HGSOC, PARPi have been approved as first and second-line maintenance therapy.[101–104] Recently, the European Medicines

Agency (EMA) approved olaparib in combination with bevacizumab (an anti-VEGF monoclonal antibody) as first-line therapy in HRD-positive platinum-sensitive HGSOC patients, using an HRD diagnostic test with demonstrated clinical validity.[11, 13, 38, 42, 101] This setting provides an opportunity to clinically validate the RAD51 assay. Regarding prostate cancer, the PARPi olaparib and rucaparib are now approved for men with metastatic disease[101, 105], but significant intra-patient variability in clinical outcomes has been observed, particularly for those patients with alterations in genes beyond BRCA2. A functional assay such as RAD51 can be relevant to assess the clinical value of less-frequent alterations in other DNA damage repair genes, e.g. PALB2, and guide patient stratification[106]. Finally, olaparib is the first targeted therapy that has been approved for gBRCA1/2-mutated pancreatic tumors that previously responded to platinum salts.[107] In this context, the RAD51 assay could be helpful to: 1) avoid platinum-based chemotherapy as selection biomarker, thus reducing toxicities for patients who may not benefit from them; 2) select patients that needed to otherwise be tested for gBRCA1/2 status, considering the low incidence of the mutations in this subset of patients; 3) increase the number of patients who may benefit from PARPi beyond those with gBRCA1/2 mutations.

We foresee that the RAD51 test will have some limitations in relationship with PARPi response: 1) it will not identify tumors whose sensitivity to PARPi lies on a DNA repair deficiency outside of the HRR core pathway (i.e. due to alterations in ATM, RNaseH2, XRCC1, ALC1); and 2) it will not identify secondary PARPi-resistance when the mechanism does not involve restoration of HRR, such as replication fork stabilization, PD-L1 induction[108]. Indeed, our studies investigating the immune-microenviroment modifications in BC animal models upon PARPi showed the upregulation of PD-L1 on tumor cells in resistant models and the increase of PD-L1 expression on T-cells in sensitive models. These data confirmed the preliminary *in vitro* [108] results of Jiao et al and paved the basis for the clinical

investigation of PARPi (as inductor of PD-L1 expression, independently of HRD status) combined to immunotherapy in PD-L1-negative TNBC.

The second part of my doctoral thesis focused on the clinical validation of the RAD51 assay on TNBC and HGSOC samples.

In the RADIMMUNE study, we confirmed that the RAD51 assay was able to identify HRD BC beyond patients harboring mutations in HHR genes. The prevalence of HRD tumors in this series was 56%, comparable with results of the retrospective analyses of the GeparSixto trial recently published by Llop-Guevara (HRD BC prevalence by Rad51 of 61%)[45]. In the RADIMMUNE study, we demonstrated that functional HRD was not a predictive factor of pCR to platinum-free chemotherapy regimens; on the other hand, Llop-Guevara et al demonstrated the predictive value of response of RAD51 to platinum salts, in the retrospective analyses of the GeparSixto trial [45]. In our cohort, functional HRD was not related with TIL extent in untreated samples; our results were in line with the paper published by Solinas et al where the authors showed the absence of the association between gBRCA1/2 mutations and TIL extent/composition[67].

For the first time, we demonstrated the prognostic value of functional HRD status in early high-risk BC patients. In our cohort, HRD patients were characterized by higher OS compared to HRP ones; interestingly, among the TIL-low population, characterized by poor prognosis, we showed that HRD/TIL-low patients had favorable OS at 5 years of 88.5%. Overall, our data paved the basis for the design of clinical trials investigating de-escalation strategies in early high-risk BC patients who underwent neoadjuvant chemotherapy.

The identification of the HRD status is of crucial importance for the identification of HGSOC patients suitable for treatment with PARPi, since HRD is associated with increased response to these therapies with respect to those who appear HR proficient[42, 109–112]. At present, Myriad represents the most

widely used test to identify the HRD status in patients with ovarian cancer. However, some limitations of Myriad and the other available HRD tests seem to exist[110]. These include the proportion of samples returned with 'unknown' status, the presence of false negative and false positives, and their high cost. Furthermore, newer approaches able to provide information of the functional activity of the pathway are required to improve the management of patients eligible to PARPi, since some patients with HRD do not respond to PARPi and platinum-based regimens[34].

Several academic laboratories are developing new approaches for HRD testing in HGSOC. In the second part of my PhD thesis, two different academic genomic HRD tests and RAD51 assay were performed and compared with Myriad, considered as a reference standard. Of note, all assays were performed on the same samples in patients enrolled in the MITO16A trial with high quality clinical data[79]. All samples were collected before the initiation of chemotherapy, representing a pure picture of baseline molecular characteristics of untreated patients with advanced ovarian cancer and allowing a correlation with the clinical outcome reported in the trial.

Overall, a high level of concordance of the two genomic approaches, namely LAB1 and LAB2, with the HRD status collected with the Myriad test was reported. This high concordance was paralleled with a very low failure rate, therefore suggesting the feasibility of LAB1 and LAB2 assays. Interestingly, the failure rate was lower than in previous studies, such as the PRIMA and PAOLA1 trials both for Myriad and LAB1 and LAB2 tests[42, 112]. This discrepancy can be likely attributed to differences in the preanalytical processing of samples that was centralized in the coordinating institution with a standardized procedure, as described previously[113]. Given the potential feasibility of LAB1 and LAB2 genomic testing, it is possible to plan future studies to further investigate the use of these assays, for instance with an ongoing prospective validation phase that is carried out on the ongoing MITO35a study, which

evaluates treatment with PARPi in patients with wild type BRCA status, in the same patient setting as of the MITO16a trial (see https://www.clinicaltrialsregister.eu/ctr-search/trial/2021-000244-21/IT).

Interestingly, Cox analysis showed that LAB1, LAB2 and Myriad data in a multivariate model including the stronger prognostic variables, such as residual disease and stage, are able to separate patients at different risk of disease progression according to HRR status, confirming that HRR is related to the outcome to platinum-based therapy.

As discussed, the assessment of functional activity of the HRR pathway would provide very relevant information for the selection of patients eligible to PARPi therapy in clinical practice. Indeed, the RAD51 functional test has already been proposed in the breast and prostate cancer settings[18, 45, 114], we performed the RAD51 assay in the largest cohort of HGSOC. A failure rate of 30% was reported for the test. We speculated that these suboptimal results, compared with the experience collected in breast cancer can be due, at least in part, to the different quality of the paraffined samples between breast biopsy and ovarian surgical samples. When the RAD51 test was evaluable, we observed discordant results both for HRD and HRD tumors by genomic assays; in some cases, we were able solve inconclusive results at genomic assays by successfully performing the RAD51. Furthermore, the RAD51 assay was able also to identify additional HRD patients compared to Myriad testing. However, due to the small number of patients, we were unable to firmly demonstrate that the RAD51 is able to better predict the response to platinum. Similarly, the small sample size may also have led to the lack of statistical significance for the prognostic ability of the combination of genomic scars and functional RAD51 testing. Of note, patients with HRP status by both genomic testing and RAD51 testing showed a trend towards shorter PFS. Indeed, the possibility of combining a genomic and a functional test to improve the management of patients with ovarian cancer is of great value. However, this hypothesis is only speculative, given the limited sample

size and will be tested in the validation phase, during which sampling will be improved to minimize pre-analytical issues.

5. Conclusion

In summary, the RAD51 assay could help to identify 1) patients harboring gBRCA1/2 or gPALB2 mutations who are likely to be PARPi-resistant and 2) patients without a germline condition in BRCA1/2 or PALB2 with HRD-positive tumors who are likely to be PARPi-sensitive. Using PDX we confirmed the superior predictive value of an immunofluorescence-based test detecting RAD51 nuclear foci in preclinical models treated with PARPi when compared to HRR-gene mutations, genomic HRD tests and platinum sensitivity.

In experimental models, olaparib elicited an antitumor immune response in PARPi-sensitive tumors. The expression of PD-L1 in tumors with poor responses to PARPi and in intratumoral lymphocytes suggested the combined use with anti-PD-L1 therapy.

The RAD51 test was able to identify HRR-altered tumors, beyond gBRCA1/2 mutations, and to select a cohort of HRD/TIL-low patients with good prognosis in a platinum-free (neo)adjuvant chemotherapy setting.

Our analysis, conducted on specimens of patients enrolled in the MITO16A trial, suggested the feasibility of RAD51 assay on HGSOC patients and the ability of the test to expand the HRD patients who may benefit from PARPi.

Given the supportive clinical data,[17, 18, 45] we proposed to continue the analytical validation and the clinical qualification of the RAD51 assay in larger cohorts of BC and HGSOC patients treated with PARPi or platinum salts.

6. Bibliography

1. Ciccia A, Elledge SJ. The DNA Damage Response: Making It Safe to Play with Knives. Mol. Cell 2011; 40(2):179–204.

2. Roy R, Chun J, Powell SN. BRCA1 and BRCA2: different roles in a common pathway of genome protection. Nat. Rev. Cancer 2011; 12(1):68–78.
3. Sun Y, McCorvie TJ, Yates LA, Zhang X. Structural basis of homologous recombination. Cell. Mol. Life Sci. 2020; 77(1):3–18.
4. Heeke AL, Pishvaian MJ, Lynce F et al. Prevalence of Homologous Recombination–Related Gene Mutations Across Multiple Cancer Types. JCO Precis. Oncol. 2018; 2(2):1–13.
5. Loibl S, Weber KE, Timms KM et al. Survival analysis of carboplatin added to an anthracycline/taxane-based neoadjuvant chemotherapy and HRD score as predictor of response – final results from GeparSixto. Ann Oncol 2018; 29(12):2341–2347.
6. Konstantinopoulos PA, Ceccaldi R, Shapiro GI, Andrea ADD. Homologous Recombination Deficiency : Exploiting the Fundamental Vulnerability of Ovarian Cancer. 2015. doi:10.1158/2159-8290.CD-15-0714.
7. O'Neil NJ, Bailey ML, Hieter P. Synthetic lethality and cancer. Nat. Rev. Genet. 2017; 18(10):613–623.
8. Lord CJ, Ashworth A. Mechanisms of resistance to therapies targeting BRCA-mutant cancers. Nat. Med. 2013; 19(11):1381–1388.
9. Shen Y, Aoyagi-Scharber M, Wang B. Trapping Poly(ADP-Ribose) Polymerase. J. Pharmacol. Exp. Ther. 2015; 353(3):446–457.
10. Pellegrino B, Herencia-Ropero A, Llop-Guevara A et al. Preclinical In Vivo Validation of the RAD51 Test for Identification of Homologous Recombination-Deficient Tumors and Patient Stratification. Cancer Res. 2022; 82(8):1646–1657.
11. Miller RE, Leary A, Scott CL et al. ESMO recommendations on predictive biomarker testing for homologous recombination deficiency and PARP inhibitor benefit in ovarian cancer. Ann. Oncol. 2020; 31(12):1606–1622.
12. Pellegrino B, Mateo J, Serra V, Balmaña J. Controversies in Oncology: homologous recombination repair deficiency (HRD) is useful for treatment decision making? ESMO Open .
13. Mirza MR, Monk BJ, Herrstedt J et al. Niraparib Maintenance Therapy in Platinum-Sensitive, Recurrent Ovarian Cancer. N. Engl. J. Med. 2016; 375(22):2154–2164.
14. Winter C, Nilsson MP, Olsson E et al. Targeted sequencing of BRCA1 and BRCA2 across a large unselected breast cancer cohort suggests that one-third of mutations are somatic. Ann. Oncol. 2016; 27(8):1532–1538.
15. Tutt A, Tovey H, Cheang MCU et al. Carboplatin in BRCA1/2-mutated and triple-negative breast cancer BRCAness subgroups: The TNT Trial. Nat. Med. 2018; 24(5):628–637.
16. Tung NM, Robson ME, Ventz S et al. TBCRC 048: Phase II Study of Olaparib for Metastatic Breast Cancer and Mutations in Homologous Recombination-Related Genes. J. Clin. Oncol. 2020; 38(36):4274–4282.
17. Chopra N, Tovey H, Pearson A et al. Homologous recombination DNA repair deficiency and PARP inhibition activity in primary triple negative breast cancer. Nat. Commun. 2020; 11(1):1–12.
18. Eikesdal HP, Yndestad S, Elzawahry A et al. Olaparib monotherapy as primary treatment in unselected triple negative breast cancer. Ann. Oncol. 2021; 32(2):240–249.
19. Telli ML, Timms KM, Reid J et al. Homologous Recombination Deficiency (HRD) Score Predicts Response to Platinum-Containing Neoadjuvant Chemotherapy in Patients with Triple-Negative Breast Cancer. Clin. Cancer Res. 2016; 22(15):3764–3773.
20. Watkins JA, Irshad S, Grigoriadis A, Tutt ANJ. Genomic scars as biomarkers of homologous recombination deficiency and drug response in breast and ovarian cancers. Breast Cancer Res. 2014. doi:10.1186/bcr3670.
21. Coleman RL, Oza AM, Lorusso D et al. Rucaparib maintenance treatment for recurrent ovarian carcinoma after response to platinum therapy (ARIEL3): a randomised, double-blind, placebo-controlled, phase 3 trial. Lancet 2018; 390(10106):1949–1961.
22. Helleday T, Eshtad S, Nik-Zainal S. Mechanisms underlying mutational signatures in human cancers. Nat. Rev. Genet. 2014; 15(9):585–598.
23. Graeser M, McCarthy A, Lord CJ et al. A Marker of Homologous Recombination Predicts Pathologic Complete Response to Neoadjuvant Chemotherapy in Primary Breast Cancer. Clin. Cancer Res. 2010;

16(24):6159–6168.
24. Naipal KAT, Verkaik NS, Ameziane N et al. Functional Ex vivo assay to select homologous recombination-deficient breast tumors for PARP inhibitor treatment. Clin. Cancer Res. 2014; 20(18):4816–4826.
25. Cruz C, Castroviejo-Bermejo M, Gutiérrez-Enriquez S et al. RAD51 foci as a functional biomarker of homologous recombination repair and PARP inhibitor resistance in germline BRCA mutated breast cancer. Ann. Oncol. 2018; 29(5):1203–1210.
26. Castroviejo-Bermejo M, Cruz C, Llop-Guevara A et al. A RAD51 assay feasible in routine tumor samples calls PARP inhibitor response beyond BRCA mutation. EMBO Mol. Med. 2018:e9172.
27. Mateo J, Carreira S, Sandhu S et al. DNA-Repair Defects and Olaparib in Metastatic Prostate Cancer. N. Engl. J. Med. 2017; 4(11):1697–1708.
28. Goodall J, Mateo J, Yuan W et al. Circulating cell-free DNA to guide prostate cancer treatment with PARP inhibition. Cancer Discov. 2017; 7(9):1006–1017.
29. Bakr A, Oing C, Köcher S et al. Involvement of ATM in homologous recombination after end resection and RAD51 nucleofilament formation. Nucleic Acids Res. 2015; 43(6):3154–3166.
30. McCabe N, Turner NC, Lord CJ et al. Deficiency in the repair of DNA damage by homologous recombination and sensitivity to poly(ADP-ribose) polymerase inhibition. Cancer Res. 2006; 66(16):8109–8115.
31. The Cancer Genome Atlas Network. Integrated Genomic Analyses of Ovarian Carcinoma. Nature 2011; 474(7353):609–615.
32. Akashi-Tanaka S, Watanabe C, Takamaru T et al. BRCAness Predicts Resistance to Taxane-Containing Regimens in Triple Negative Breast Cancer During Neoadjuvant Chemotherapy. Clin. Breast Cancer 2015; 15(1):80–85.
33. Robinson D, Van Allen EM, Wu YM et al. Integrative clinical genomics of advanced prostate cancer. Cell 2015; 1(1):1–12.
34. Hoppe MM, Sundar R, Tan DSP, Jeyasekharan AD. Biomarkers for Homologous Recombination Deficiency in Cancer. JNCI J. Natl. Cancer Inst. 2018; 110(7):704–713.
35. Heeke A, Lynce F, Baker T et al. Prevalence of Homologous Recombination Deficiency (HRD) Among All Tumor Types. J. Clin. Oncol. 2017; 15_suppl(35):1502–1502.
36. Connor MJO. Targeting the DNA Damage Response in Cancer. Mol. Cell 2015; 60(4):547–560.
37. Ledermann JA, Harter P, Gourley C et al. Overall survival in patients with platinum-sensitive recurrent serous ovarian cancer receiving olaparib maintenance monotherapy: an updated analysis from a randomised, placebo-controlled, double-blind, phase 2 trial. Lancet Oncol. 2016; 17(11):1579–1589.
38. Swisher EM, Lin KK, Oza AM et al. Rucaparib in relapsed, platinum-sensitive high-grade ovarian carcinoma (ARIEL2 Part 1): an international, multicentre, open-label, phase 2 trial. Lancet Oncol. 2017; 18(1):75–87.
39. Robson M, Im S-A, Senkus E et al. Olaparib for Metastatic Breast Cancer in Patients with a Germline *BRCA* Mutation. N. Engl. J. Med. 2017:NEJMoa1706450.
40. Litton JK, Rugo HS, Ettl J et al. Talazoparib in Patients with Advanced Breast Cancer and a Germline BRCA Mutation. N. Engl. J. Med. 2018; 379(8):753–763.
41. https://www.ema.europa.eu/medicines/human/. .
42. Ray-Coquard I, Pautier P, Pignata S et al. Olaparib plus Bevacizumab as First-Line Maintenance in Ovarian Cancer. N. Engl. J. Med. 2019; 381(25):2416–2428.
43. Litton JK, Scoggins M, Hess KR et al. Neoadjuvant talazoparib (TALA) for operable breast cancer patients with a BRCA mutation (BRCA+). J. Clin. Oncol. 2018; 36(15_suppl):508–508.
44. Isakoff SJ, Mayer EL, He L et al. TBCRC009: A multicenter phase II clinical trial of platinum monotherapy with biomarker assessment in metastatic triple-negative breast cancer. J. Clin. Oncol. 2015; 33(17):1902–1909.
45. Llop-Guevara A, Loibl S, Villacampa G et al. Association of RAD51 with homologous recombination deficiency (HRD) and clinical outcomes in untreated triple-negative breast cancer (TNBC): analysis of the GeparSixto randomized clinical trial. Ann. Oncol. Off. J. Eur. Soc. Med. Oncol. 2021.

46. Pellegrino B, Musolino A, Llop-Guevara A et al. Homologous Recombination Repair Deficiency and the Immune Response in Breast Cancer: A Literature Review, 2020; 13(2):410–422.
47. Parkes EE, Walker SM, Taggart LE et al. Activation of STING-Dependent Innate Immune Signaling By S-Phase-Specific DNA Damage in Breast Cancer. 2017; 109:1–10.
48. Dunphy G, Flannery SM, Almine JF et al. Non-canonical Activation of the DNA Sensing Adaptor STING by ATM and IFI16 Mediates NF-κB Signaling after Nuclear DNA Damage. Mol. Cell 2018; 71(5):745-760.e5.
49. Pantelidou C, Sonzogni O, de Oliveira Taveira M et al. PARP inhibitor efficacy depends on CD8+ T cell recruitment via intratumoral STING pathway activation in BRCA-deficient models of triple-negative breast cancer. Cancer Discov. 2019:CD-18-1218.
50. Pellegrino B, Llop-Guevara A, Cruz C et al. 18PDissecting the antitumor immune response upon PARP inhibition in homologous recombination repair (HRR)-deficient tumors. Ann. Oncol. 2018. doi:10.1093/annonc/mdy493.016.
51. Solinas C, Ceppi M, Lambertini M et al. Tumor-infiltrating lymphocytes in patients with HER2-positive breast cancer treated with neoadjuvant chemotherapy plus trastuzumab, lapatinib or their combination: A meta-analysis of randomized controlled trials. Cancer Treat. Rev. 2017; 57(May):8–15.
52. Denkert C, von Minckwitz G, Darb-Esfahani S et al. Tumour-infiltrating lymphocytes and prognosis in different subtypes of breast cancer: a pooled analysis of 3771 patients treated with neoadjuvant therapy. Lancet Oncol. 2018; 19(1):40–50.
53. Salgado R, Loi S. Tumour infiltrating lymphocytes in breast cancer: increasing clinical relevance. Lancet Oncol. 2018; 19(1):3–5.
54. Solinas C, Carbognin L, De Silva P et al. Tumor-infiltrating lymphocytes in breast cancer according to tumor subtype: Current state of the art. Breast 2017; 35:142–150.
55. Schmid P, Adams S, Rugo HS et al. Atezolizumab and Nab-Paclitaxel in Advanced Triple-Negative Breast Cancer. N. Engl. J. Med. 2018; 379(22):2108–2121.
56. Loi S, Giobbe-Hurder A, Gombos A et al. Phase Ib/II study evaluating safety and efficacy of pembrolizumab and trastuzumab in patients with trastuzumab-resistant HER2-positive metastatic breast cancer: Results from the PANACEA (IBCSG 45-13/BIG 4-13/KEYNOTE-014) study. Cancer Res. 2017.
57. Schmid P, Cruz C, Braiteh FS et al. Abstract 2986: Atezolizumab in metastatic TNBC (mTNBC): Long-term clinical outcomes and biomarker analyses. Cancer Res. 2017; 77(13 Supplement):2986–2986.
58. Loi S, Giobbe-Hurder A, Gombos A et al. Abstract GS2-06: Phase Ib/II study evaluating safety and efficacy of pembrolizumab and trastuzumab in patients with trastuzumab-resistant HER2-positive metastatic breast cancer: Results from the PANACEA (IBCSG 45-13/BIG 4-13/KEYNOTE-014) study. Cancer Res. 2018; 78(4 Supplement):GS2-06-GS2-06.
59. Denkert C, Wienert S, Poterie A et al. Standardized evaluation of tumor-infiltrating lymphocytes in breast cancer: results of the ring studies of the international immuno-oncology biomarker working group. Mod. Pathol. 2016; 29(10):1155–1164.
60. Dieci M, Radosevic-Robin N, Fineberg S et al. Seminars in Cancer Biology Update on tumor-in fi ltrating lymphocytes (TILs) in breast cancer , including recommendations to assess TILs in residual disease after neoadjuvant therapy and in carcinoma in situ : A report of the International Immuno- Oncol. Semin. Cancer Biol. 2017; (September):1–10.
61. Hendry S, Salgado R, Gevaert T et al. Assessing Tumor-infiltrating Lymphocytes in Solid Tumors: A Practical Review for Pathologists and Proposal for a Standardized Method from the International Immunooncology Biomarkers Working Group: Part 1: Assessing the Host Immune Response, TILs in Invasi. Adv. Anat. Pathol. 2017; 24(5):235–251.
62. Hendry S, Salgado R, Gevaert T et al. Assessing Tumor-infiltrating Lymphocytes in Solid Tumors. Adv. Anat. Pathol. 2017; 24(5):235–251.
63. Stoppa-Lyonnet D. The biological effects and clinical implications of BRCA mutations: where do we go from here? Eur. J. Hum. Genet. 2016; 24(S1):S3–S9.
64. Alexandrov LB, Nik-Zainal S, Wedge DC et al. Signatures of mutational processes in human cancer. Nature 2013; 500(7463):415–421.

65. Nik-Zainal S, Davies H, Staaf J et al. Landscape of somatic mutations in 560 breast cancer whole-genome sequences. Nature 2016; 534(7605):47–54.
66. Turner N, Tutt A, Ashworth A. Hallmarks of "BRCAness" in sporadic cancers. Nat. Rev. Cancer 2004; 4(10):814–819.
67. Solinas C, Marcoux D, Garaud S et al. BRCA gene mutations do not shape the extent and organization of tumor infiltrating lymphocytes in triple negative breast cancer. Cancer Lett. 2019; 450:88–97.
68. Nolan E, Savas P, Policheni AN et al. Combined immune checkpoint blockade as a therapeutic strategy for BRCA1-mutated breast cancer. Sci. Transl. Med. 2017; 4922(June):1–13.
69. Thorsson V, Gibbs DL, Brown SD et al. The Immune Landscape of Cancer. Immunity 2018; 48(4):812-830.e14.
70. Dunn GP, Old LJ, Schreiber RD. The Three Es of Cancer Immunoediting. Annu. Rev. Immunol. 2004; 22(1):329–360.
71. Davies H, Glodzik D, Morganella S et al. HRDetect is a predictor of BRCA1 and BRCA2 deficiency based on mutational signatures. Nat. Med. 2017; 23(4):517–525.
72. Sztupinszki Z, Diossy M, Krzystanek M et al. Migrating the SNP array-based homologous recombination deficiency measures to next generation sequencing data of breast cancer. npj Breast Cancer 2018 41 2018; 4(1):1–4.
73. Bruna A, Rueda OM, Greenwood W et al. A Biobank of Breast Cancer Explants with Preserved Intra-tumor Heterogeneity to Screen Anticancer Compounds. Cell 2016; 167(1):260-274.e22.
74. Ter Brugge P, Kristel P, van der Burg E et al. Mechanisms of Therapy Resistance in Patient-Derived Xenograft Models of BRCA1-Deficient Breast Cancer. J. Natl. Cancer Inst. 2016.
75. Ballabeni A, Zamponi R, Moore JK et al. Geminin deploys multiple mechanisms to regulate Cdt1 before cell division thus ensuring the proper execution of DNA replication. Proc. Natl. Acad. Sci. U. S. A. 2013; 110(30):E2848-53.
76. Li H. Aligning sequence reads, clone sequences and assembly contigs with BWA-MEM. arXiv: Genomics 2013. doi:10.6084/M9.FIGSHARE.963153.V1.
77. Lai Z, Markovets A, Ahdesmaki M et al. VarDict: A novel and versatile variant caller for next-generation sequencing in cancer research. Nucleic Acids Res. 2016. doi:10.1093/nar/gkw227.
78. Riester M, Singh AP, Brannon AR et al. PureCN: Copy number calling and SNV classification using targeted short read sequencing. Source Code Biol. Med. 2016; 11(1):1–13.
79. Daniele G, Raspagliesi F, Scambia G et al. Bevacizumab, carboplatin, and paclitaxel in the first line treatment of advanced ovarian cancer patients: the phase IV MITO-16A/MaNGO-OV2A study. Int. J. Gynecol. Cancer 2021; 31(6):875–882.
80. Jaspers JE, Kersbergen A, Boon U et al. Loss of 53BP1 causes PARP inhibitor resistance in BRCA1-mutated mouse mammary tumors. Cancer Discov. 2013; 3(1):68–81.
81. Xu G, Ross Chapman J, Brandsma I et al. REV7 counteracts DNA double-strand break resection and affects PARP inhibition. Nature 2015; 521(7553):541–544.
82. Dev H, Chiang TWW, Lescale C et al. Shieldin complex promotes DNA end-joining and counters homologous recombination in BRCA1-null cells. Nat. Cell Biol. 2018; 20(8):954–965.
83. Drost R, Dhillon KK, Van Der Gulden H et al. BRCA1185delAG tumors may acquire therapy resistance through expression of RING-less BRCA1. J. Clin. Invest. 2016; 126(8):2903–2918.
84. Wang Y, Bernhardy AJ, Cruz C et al. The BRCA1-Δ11q alternative splice isoform bypasses germline mutations and promotes therapeutic resistance to PARP inhibition and cisplatin. Cancer Res. 2016; 76(9):2778–2790.
85. Wang Y, Bernhardy AJ, Nacson J et al. BRCA1 intronic Alu elements drive gene rearrangements and PARP inhibitor resistance. Nat. Commun. 2019; 10(1):1–12.
86. Coussy F, El-Botty R, Château-Joubert S et al. BRCAness, SLFN11, and RB1 loss predict response to topoisomerase I inhibitors in triple-negative breast cancers. Sci. Transl. Med. 2020; 12(532):eaax2625.
87. Bunting SF, Callén E, Kozak ML et al. BRCA1 Functions Independently of Homologous Recombination in DNA Interstrand Crosslink Repair. Mol. Cell 2012; 46(2):125–135.
88. Farkkila A, Rodríguez A, Oikkonen J et al. Heterogeneity and clonal evolution of acquired PARP inhibitor

resistance in TP53- And BRCA1-deficient cells. Cancer Res. 2021; 81(10):2774–2787.
89. Sato H, Niimi A, Yasuhara T et al. DNA double-strand break repair pathway regulates PD-L1 expression in cancer cells. Nat. Commun. 2017; 8(1):1751.
90. Ghosh R, Roy S, Franco S. PARP1 depletion induces RIG-I-dependent signaling in human cancer cells. PLoS One 2018; 13(3):e0194611.
91. Horton JK, Stefanick DF, Prasad R et al. Base excision repair defects invoke hypersensitivity to PARP inhibition. Mol. Cancer Res. 2014; 12(8):1128–1139.
92. Zimmermann M, Murina O, Reijns MAM et al. CRISPR screens identify genomic ribonucleotides as a source of PARP-trapping lesions. Nature 2018; 559(7713):285–289.
93. Verma P, Zhou Y, Cao Z et al. ALC1 links chromatin accessibility to PARP inhibitor response in homologous recombination-deficient cells. Nat. Cell Biol. 2021; 23(2):160–171.
94. Hewitt G, Borel V, Segura-Bayona S et al. Defective ALC1 nucleosome remodeling confers PARPi sensitization and synthetic lethality with HRD. Mol. Cell 2021; 81(4):767-783.e11.
95. Robson M, Im S-A, Senkus E et al. Olaparib for Metastatic Breast Cancer in Patients with a Germline BRCA Mutation. N. Engl. J. Med. 2017; 377(6):523–533.
96. Gruber JJ, Afghahi A, Hatton A et al. Talazoparib beyond BRCA: A phase II trial of talazoparib monotherapy in BRCA1 and BRCA2 wild-type patients with advanced HER2-negative breast cancer or other solid tumors with a mutation in homologous recombination (HR) pathway genes. . J. Clin. Oncol. 2019; 37(15_suppl):3006–3006.
97. Fasching PA, Link T, Hauke J et al. Neoadjuvant paclitaxel/olaparib in comparison to paclitaxel/carboplatinum in patients with HER2-negative breast cancer and homologous recombination deficiency (GeparOLA study). Ann. Oncol. 2021; 32(1):49–57.
98. Tutt ANJ, Garber JE, Kaufman B et al. Adjuvant Olaparib for Patients with BRCA1 - or BRCA2 -Mutated Breast Cancer. N. Engl. J. Med. 2021; 384(25):2394–2405.
99. Hahnen E, Lederer B, Hauke J et al. Germline Mutation Status, Pathological Complete Response, and Disease-Free Survival in Triple-Negative Breast Cancer. JAMA Oncol. 2017; 3(10):1378.
100. Postel-Vinay S, Soria JC. ERCC1 as Predictor of Platinum Benefit in Non-Small-Cell Lung Cancer. J. Clin. Oncol. 2017; 35(4):384–386.
101. Lynparza | European Medicines Agency. [https://www.ema.europa.eu/en/medicines/human/EPAR/lynparza].
102. Zejula, INN-niraparib. [https://www.ema.europa.eu/en/medicines/human/EPAR/zejula].
103. Rubraca | European Medicines Agency. [https://www.ema.europa.eu/en/medicines/human/EPAR/rubraca].
104. Banerjee S, Moore KN, Colombo N et al. 811MO Maintenance olaparib for patients (pts) with newly diagnosed, advanced ovarian cancer (OC) and a BRCA mutation (BRCAm): 5-year (y) follow-up (f/u) from SOLO1. Ann. Oncol. 2020; 31:S613.
105. Anscher MS, Chang E, Gao X et al. FDA Approval Summary: Rucaparib for the Treatment of Patients with Deleterious BRCA-Mutated Metastatic Castrate-Resistant Prostate Cancer. Oncologist 2021; 26(2):139–146.
106. Carreira S, Porta N, Arce-Gallego S et al. Biomarkers Associating with PARP Inhibitor Benefit in Prostate Cancer in the TOPARP-B Trial. Cancer Discov. 2021; 11(11):2812–2827.
107. Golan T, Hammel P, Reni M et al. Maintenance Olaparib for Germline BRCA -Mutated Metastatic Pancreatic Cancer . N. Engl. J. Med. 2019; 381(4):317–327.
108. Jiao S, Xia W, Yamaguchi H et al. PARP inhibitor upregulates PD-L1 expression and enhances cancer-associated immunosuppression. Clin. Cancer Res. 2017; 23(14):3711–3720.
109. Telli ML, Stover DG, Loi S et al. Homologous recombination deficiency and host anti-tumor immunity in triple-negative breast cancer. Breast Cancer Res. Treat. 2018; 171(1):21–31.
110. Ngoi NYL, Tan DSP. The role of homologous recombination deficiency testing in ovarian cancer and its clinical implications: do we need it? ESMO open 2021. doi:10.1016/J.ESMOOP.2021.100144.
111. Takamatsu S, Brown JB, Yamaguchi K et al. Utility of Homologous Recombination Deficiency Biomarkers Across Cancer Types. JCO Precis. Oncol. 2022. doi:10.1200/po.22.00085.
112. González-Martín A, Pothuri B, Vergote I et al. Niraparib in Patients with Newly Diagnosed Advanced

Ovarian Cancer. N. Engl. J. Med. 2019; 381(25):2391–2402.
113. Califano D, Russo D, Scognamiglio G et al. Ovarian Cancer Translational Activity of the Multicenter Italian Trial in Ovarian Cancer (MITO) Group: Lessons Learned in 10 Years of Experience. Cells 2020. doi:10.3390/CELLS9040903.
114. Carreira S, Porta N, Arce-Gallego S et al. Biomarkers Associating with PARP Inhibitor Benefit in Prostate Cancer in the TOPARP-B Trial. Under Rev. .

7. Figures

Figure 1. Homologous recombination repair pathway (adapted from Roy et al)[2]. Several proteins are involved, such as BRCA1 and BRCA2, that if mutated in the germline, are responsible for the Hereditary Breast and Ovarian Cancer Syndrome (HBOCS). Almost 50% of Triple negative Breast Cancer (TNBC) harbor a mutation in the genes involved in HRR pathway.

Figure 2. Defective DNA repair as a therapeutic target

Figure 3. Canonical STING pathway activation. Elevated levels of basal DNA damage results in the increase of cytosolic DNA (cDNA) which induces an activation of cGAS and, consequently, the translocation of STING from the endoplasmic reticulum to the nucleus. There, STING leads to the transcription of several IFN type I -related genes by IRF3 activation, thus inducing the production of IFN type I and chemo-attractive cytokines, i.e. chemokine (C-X-C motif) ligand 10 (CXCL10) and chemokine (C-C motif) ligand 5 (CCL5). This leads to NK cell, M1-like macrophage and both T and B-lymphocyte recruitment in an Ag-independent manner.

Figure 4. Alternative STING pathway activation. High levels of DNA damage also activate the so called “alternative STING pathway” by ATM-TRAF6, inducing the production of IL-6 and Transforming Growth Factor (TGF)-β generating the recruitment of pro-tumor M2-like macrophages and regulatory T cells (Tregs). Furthermore, ATM-TRAF6 activates the transcription factor Nuclear Factor kB (NFkB) and induces tumor cell upregulation of PD-L1 that may elicit immune-escape. Besides this mechanism, IFN type I itself (secreted upon STING activation) is the main factor inducing transcription and expression of PD-L1.

Figure 5. Establishing a biobank of patient-derived laboratory models. Study design depicting the generation of PDX from BC, HGSOC and PaC, and PDC from BC. 109 PDX were established from patient tumor samples. 14 PDC were generated from the corresponding PDX.

Figure 6. Antitumor activity of PARPi in PDX. A) Waterfall plot showing the best response to the PARPi olaparib or niraparib in 109 PDX, as percentage of tumor volume change, compared to the tumor volume on day 1. +20%, −30%, -95% are marked by dotted lines to indicate the range of PD, SD, PR, CR, respectively. The legend summarizes the RAD51 score (A), the genomic HRD score (B) (based on Myriad myChoice or HRDetect) and (C) the tumor type. B) Pie charts indicating the distribution of HRR functional status and HRR alterations in 96 PDX (excluding models of acquired resistance). C) Pie charts indicating the distribution of PARPi resistance mechanisms in 69 HRR-altered tumors (including models of acquired resistance).

Figure 7. RAD51 functional assay predicts PARPi response in PDX. A) Genomic HRD score in PARPi-sensitive and resistant models (n=41), measured with Myriad myChoice. B) Comparison of the RAD51 score with the genomic HRD score as in panel B (n=41). C) Distribution of the RAD51 score in relationship to PARPi response (n=109). D) Comparison of ROC curves for the RAD51 score and Myriad myChoice score for PARPi response in PDX (n=41).

Figure 8. Antitumor activity of cisplatin in PDX. A) Waterfall plot showing the best response to cisplatin in 56 PDX, as the percentage of tumor volume change compared to the tumor volume on day 1. +20%, −30%, -95% are marked by dotted lines to indicate the range of PD, SD, PR, CR, respectively. B) Distribution of the RAD51 score in platinum-sensitive and resistant models (n=56).

Figure 9. Homologous recombination repair functionality and PARPi sensitivity is concordant in patient, PDX and PDC. A) RAD51 scores in PDX and in patient's tumor samples concurrent to the PDX establishment. B) RAD51 in PDX and corresponding PDC treated with PARPi or vehicle. C)

Representation of the logarithm of the half maximal inhibitory concentration (IC50) of PDCs treated with olaparib in comparison to the *in vivo* sensitivity. D) Bright-field microscopic images showing one PARPi-sensitive model (PDC405) and one PARPi-resistant model (PDC270) untreated (control) and treated with olaparib 1 μM for 14 days.

Figure 10. PD-L1 positive cells in untreated and PARPi-treated PDX by IHC.

Figure 11. CD45 positive cells in untreated and PARPi treated PDXs by IHC.

Figure 12. Differential expression analysis between sensitive and resistant PDXs by RnaSeq.

Figure 13. Correlation between pCR, DFS and OS in high risk early BC.

Figura 14. Correlation between HRD status by RAD51 and HRR alterations in high risk early BC.

Figura 15. Correlation between HRD status by RAD51, DFS and OS in high risk early BC.

Figure 16. Correlation between pCR and RAD51 score.

Figure 17. DFS and OS by HRD status in high risk no pCR early BC.

Figure 18. DFS and OS according to HRD status and TIL extent.

Figure 19. Study flow chart.

Figure 20. Progression free survival Kaplan Meier curves by HRR status (a: Myriad, b: LAB1, c: LAB2, d: RAD51).

Figure 21. Overall survival Kaplan Meier curves by HRR status (a: Myriad, b: LAB1, c: LAB2, d: RAD51).

Figure 22. Overall PFS Kaplan Meier curves by combined Myriad and Rad 51 tests.

Tables

Table 1. Efficacy of PARPi according to HRD status in ovarian cancer.

Clinical trial	Drug	Setting	Study population	HRD role
ARIEL-2	Rucaparib	Monotherapy	Relapsed, platinum-sensitive ovarian cancer	Higher efficacy in *g*BRCA1/2-mutated and/or

				LOH-high compared to LOH-low tumors. Not powered to show a difference between LOH-high and LOH-low tumors
ARIEL-3	Rucaparib	Maintenance therapy	Platinum-sensitive ovarian cancer	Efficacy regardless of LOH-status.
NOVA-trial	Niraparib	Maintenance therapy	Platinum-sensitive ovarian cancer	Efficacy regardless of HRD-status.

Table 2. Efficacy of PARPi according to HRD status in breast cancer.

Clinical trial	**Drug**	**Setting**	**Study population**	**HRD role**
PrECOG 0105 Cisplatin-1 trial Cisplatin-2 trial	Platinum salts	Neoadjuvant setting	Untreated patients	HRD-positive patients had higher complete pathologic response
Gepar-Sixto trial	Carboplatin	Neoadjuvant setting	Untreated patients	HRD-positive patients have a better prognosis compared to HRD-negative ones. No robust conclusions can be reached about the predictive role of HRD regarding carboplatin

TBCRC009 trial	Platinum salts	Advanced setting	First or second-line treatment	Higher HRD scores were reported in responding patients, independent of BRCA1/2 mutational status.
TNT trial	Carboplatinum	Advanced setting	First line treatment	ORR did not correlate with HRD-score of the primary tumors.

Table 3. Test performance values for the indicated HRD biomarkers predicting PARPi response.

Biomarkers of PARPi response	**BRCA1/2, PALB2 mutations (n=109)**	**Low BRCA1 mRNA/foci (n=108)**	**Genomic HRD score (≥42) (n=41)**	**RAD51 score (≤10) (n=109)**	**Platinum response (n=56)**
Sensitivity	76%	38%	100%	90%	73%
Specificity	64%	81%	59%	98%	49%
PPV	43%	42%	50%	93%	26%
NPV	88%	78%	100%	96%	88%
Accuracy	67%	69%	71%	95%	54%

Table 4. Test performance values for the indicated HRD biomarkers predicting cisplatin response.

Biomarkers of platinum response	**BRCA1/2, PALB2 mutations (n=56)**	**Low BRCA1 mRNA/foci (n=56)**	**RAD51 score (≤10) (n=56)**
Sensitivity	68%	42%	48%
Specificity	52%	88%	84%

PPV	64%	81%	79%
NPV	57%	55%	57%
Accuracy	61%	63%	64%

Table 5. Baseline characteristics of HGSOC patients (n=100).

Features	n (%)
Median age (IQR)	57.8 (50.0; 66.3)
Age category	
<65	70 (70.0)
≥65	30 (30.0)
ECOG performance status	
0	80 (80.0)
1-2	20 (20.0)
Residual disease	
None	36 (36.0)
≤ 1 cm	25 (25.0)
> 1 cm/ not operated	39 (39.0)
FIGO stage	
IIIB	9 (9.0)
IIIC	72 (72.0)
IV	19 (19.0)
Histology	
Serous G3	98 (98.0)
Endometrioid G3	2 (2.0)

Table 6. Outcomes by HRR status, data for all assays and Myriad

	Myriad		**LAB1**		**LAB2**		**LAB3**	
Eligible for RECIST assessment	59		63		62		47	
	HRD	**HRP**	**HRD**	**HRP**	**HRD**	**HRP**	**HRD**	**HRP**
Response Rate (CI 95%)	82.4% (64.8%-92.2%)	60% (38.8%-78.0%)	84.2% (68.1%-93.0%)	56.0% (35.3%-74.8%)	75.8% (57.4%-87.9%)	65.5% (45.7%-81.0%)	90.9% (46.3%-99.1%)	72.2% (54.7%-84.8%)
Eligible for Survival analysis	94		97		97		69	
	HRD	**HRP**	**HRD**	**HRP**	**HRD**	**HRP**	**HRD**	**HRP**
Median PFS (CI 95%)	18.6 (12.0-22.3)	20.2 (17.0-25.3)	19.8 (16.3-24.2)	18.6 (12.0-22.6)	20.8 (16.3-27.5)	17.7 (12.0-22.1)	19.2 (15.8-22.1)	17.7 (9.9-25.1)
Median OS (CI 95%)	40.6 (27.3-.)	41.1 (34.8-.)	61 (37.9-.)	39.7 (24.7-.)	41.1 (34.8-42.0)	39.7 (24.7-.)	37.9 (27.2-.)	39.7 (17.9-.)

Figure 1

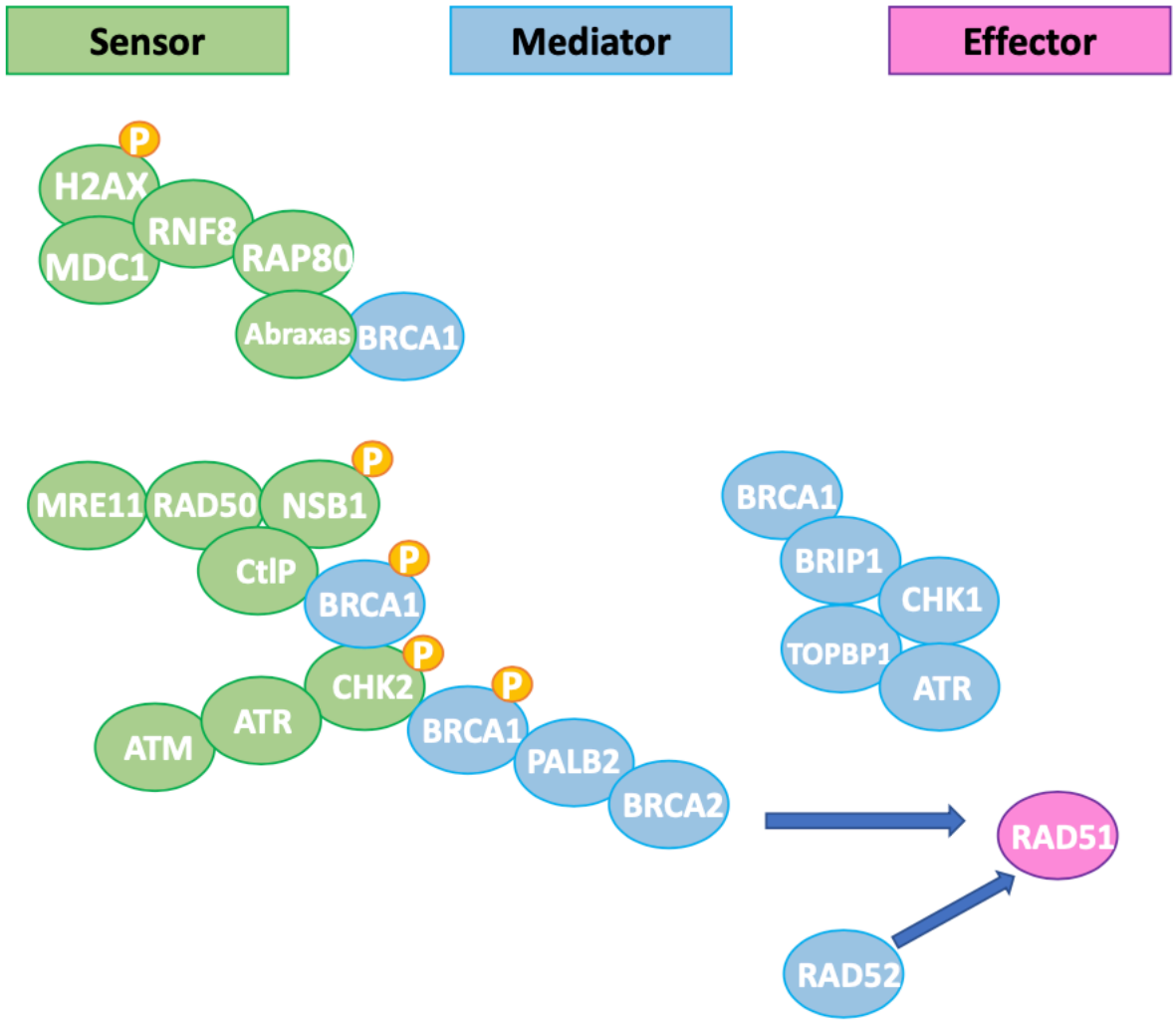
Sensor
Mediator
Effector
P
H2AX
RNF8
MDC1
RAP80
Abraxas
BRCA1
MRE11
RAD50
NSB1
P
CtIP
BRCA1
P
CHK2
P
ATR
ATM
BRCA1
PALB2
BRCA2
BRCA1
BRIP1
CHK1
TOPBP1
ATR
RAD51
RAD52

Figure 2

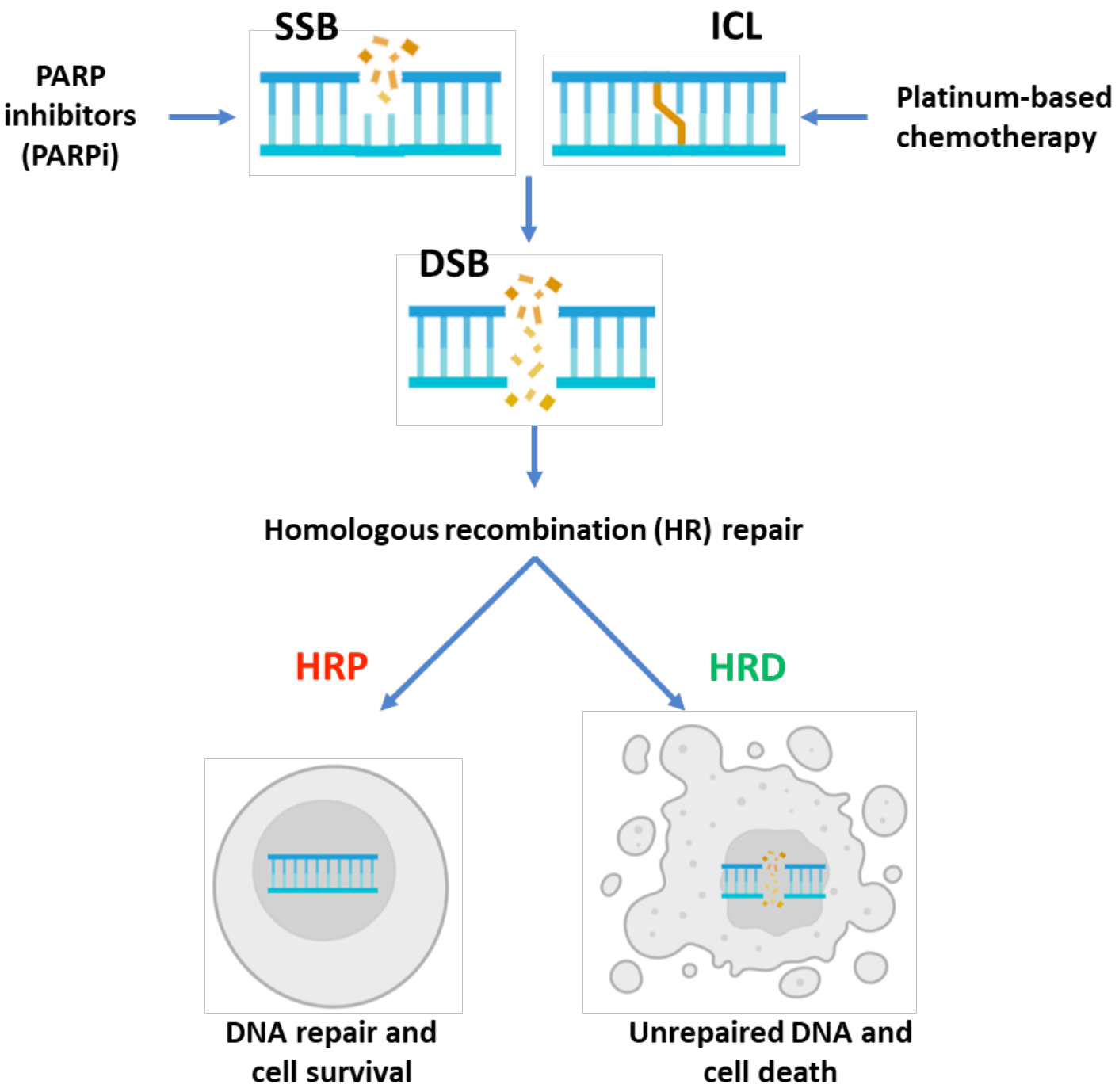
SSB
ICL
PARP inhibitors (PARPi)
Platinum-based chemotherapy
DSB
Homologous recombination (HR) repair
HRP
HRD
DNA repair and cell survival
Unrepaired DNA and cell death

Figure 3

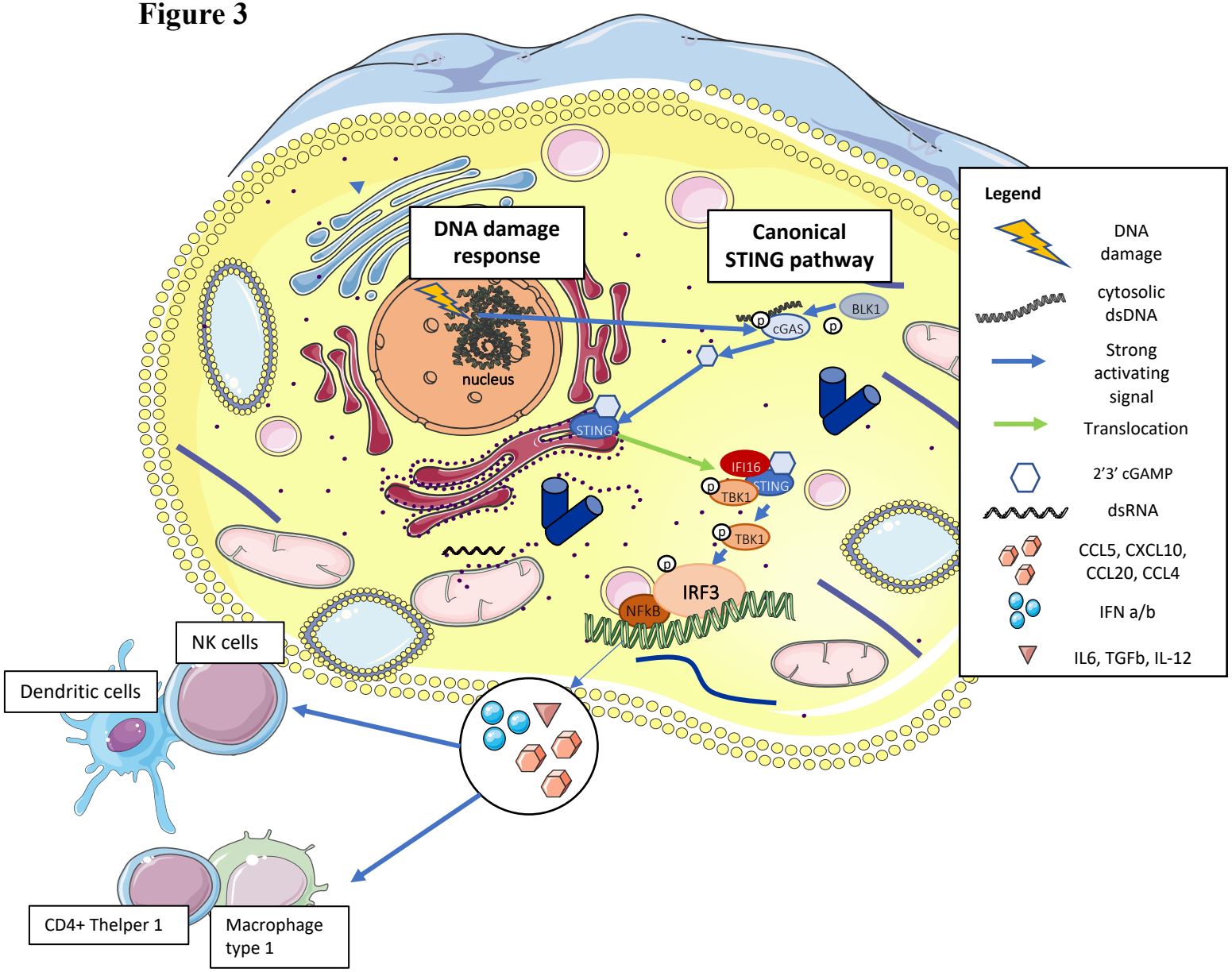
DNA damage response
Canonical STING pathway
nucleus
cGAS
BLK1
STING
IFI16
TBK1
IRF3
NFkB
NK cells
Dendritic cells
CD4+ Thelper 1
Macrophage type 1
Legend
DNA damage
cytosolic dsDNA
Strong activating signal
Translocation
2'3' cGAMP
dsRNA
CCL5, CXCL10, CCL20, CCL4
IFN a/b
IL6, TGFb, IL-12

Figure 4

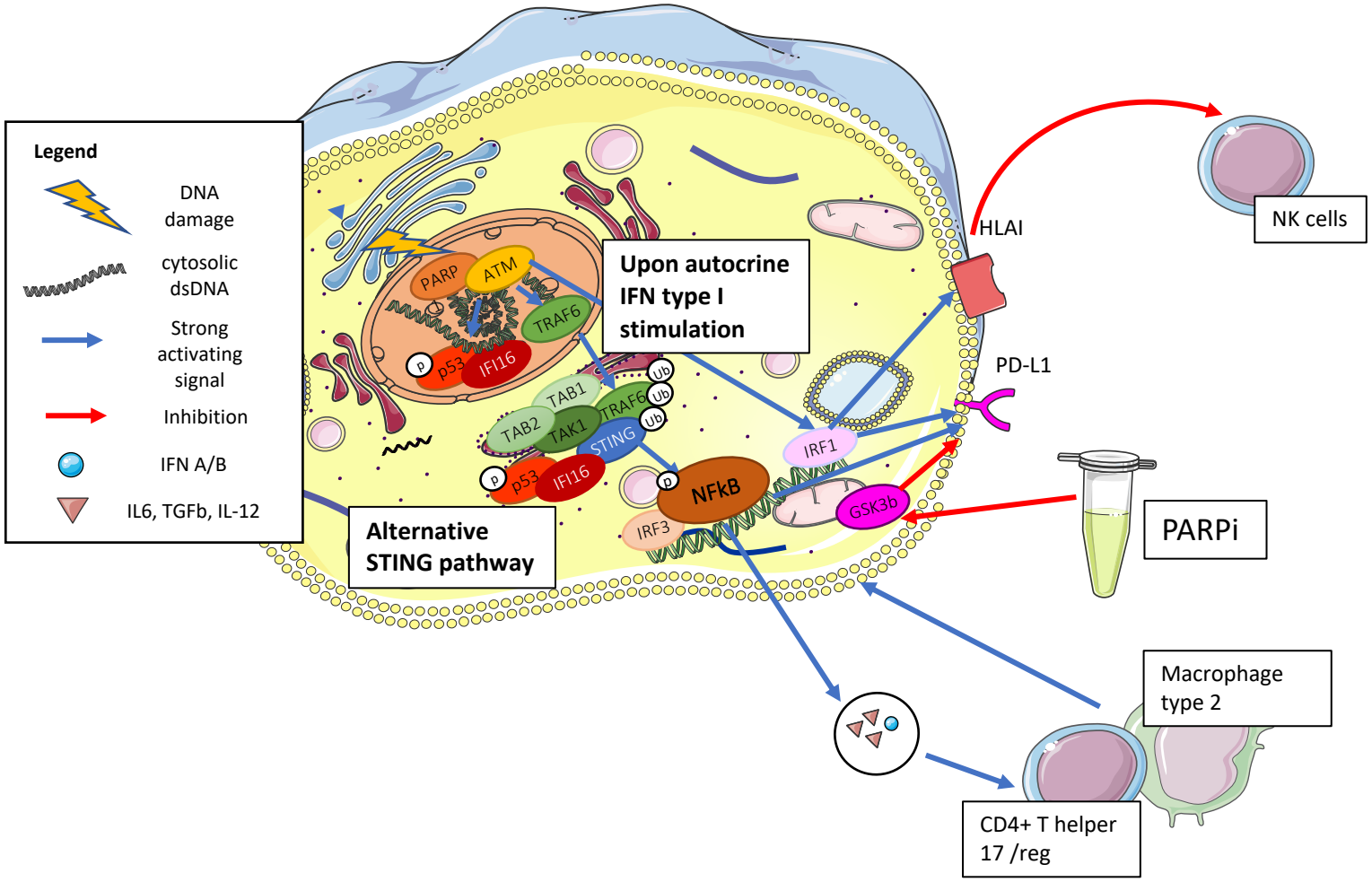
Legend
DNA damage
cytosolic dsDNA
Strong activating signal
Inhibition
IFN A/B
IL6, TGFb, IL-12
PARP
ATM
TRAF6
p
p53
IFI16
Upon autocrine IFN type I stimulation
TAB1
TAB2
TAK1
TRAF6
STING
Ub
IRF1
GSK3b
NFkB
IRF3
Alternative STING pathway
HLAI
PD-L1
NK cells
PARPi
Macrophage type 2
CD4+ T helper 17 /reg

Figure 5

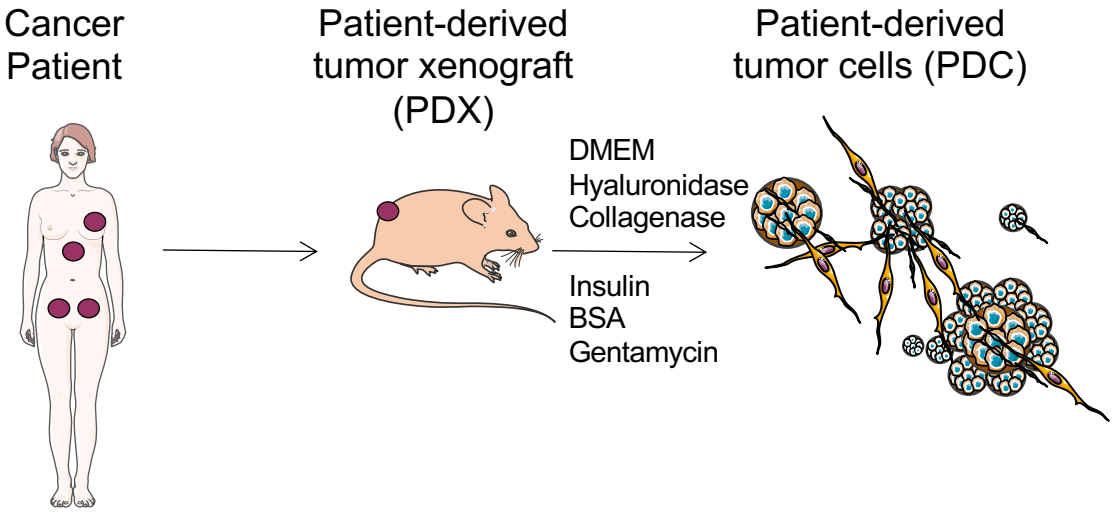
Cancer Patient
Patient-derived tumor xenograft (PDX)
Patient-derived tumor cells (PDC)
DMEM
Hyaluronidase
Collagenase
Insulin
BSA
Gentamycin

Figure 6

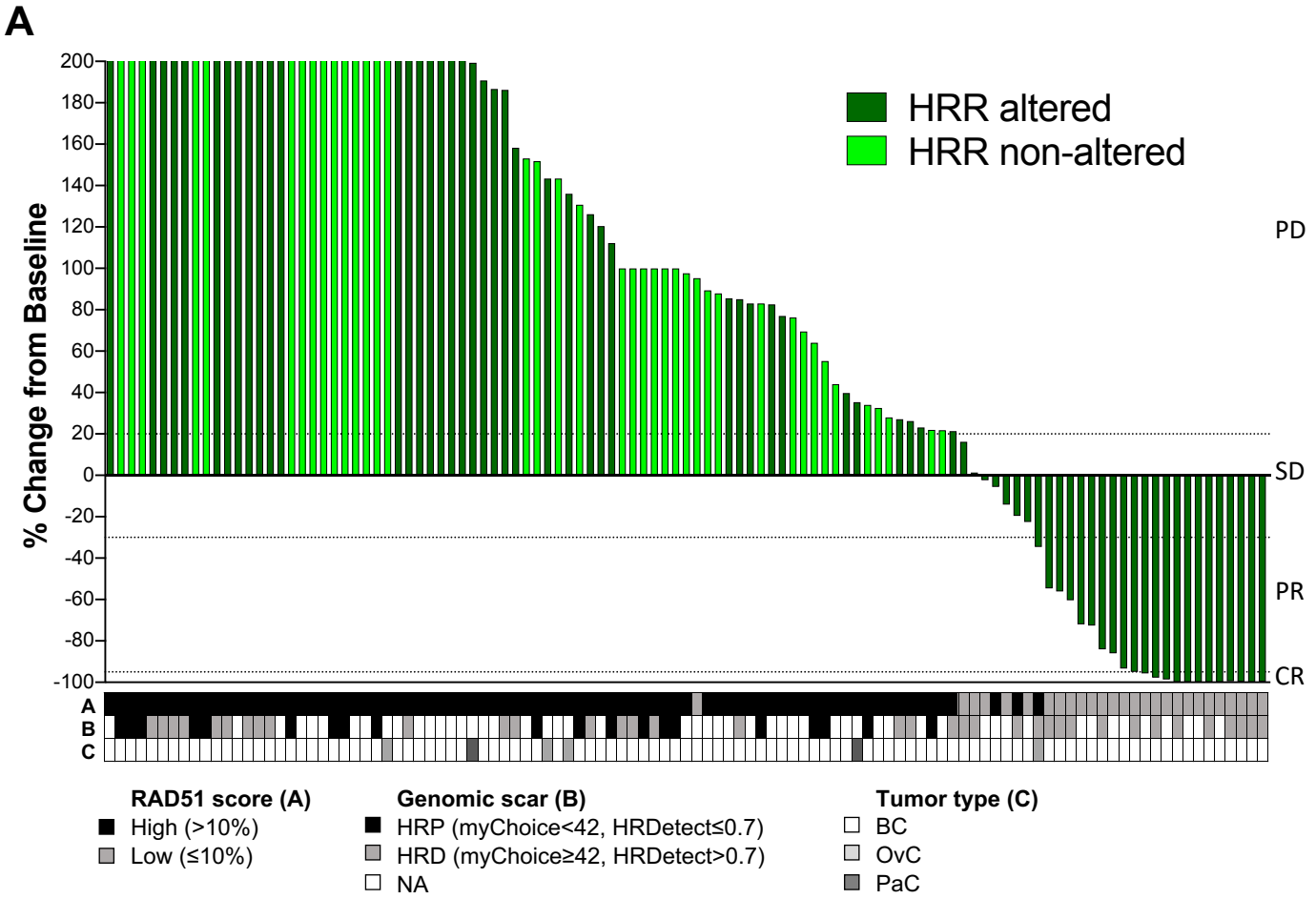
A
% Change from Baseline
HRR altered
HRR non-altered
PD
SD
PR
CR
A
B
C
RAD51 score (A)
High (>10%)
Low (≤10%)
Genomic scar (B)
HRP (myChoice<42, HRDetect≤0.7)
HRD (myChoice≥42, HRDetect>0.7)
NA
Tumor type (C)
BC
OvC
PaC

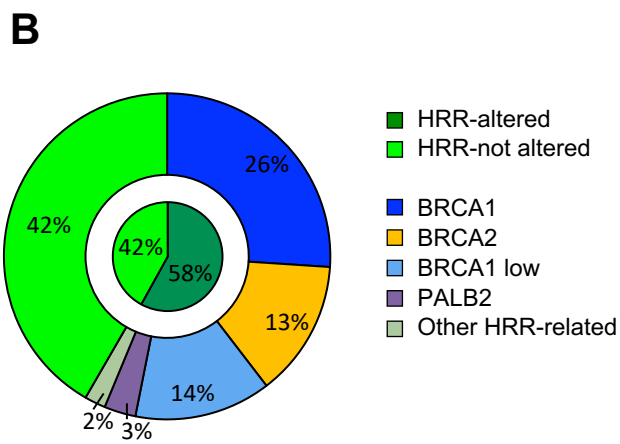
B
26%
13%
14%
3%
2%
42%
42%
58%
HRR-altered
HRR-not altered
BRCA1
BRCA2
BRCA1 low
PALB2
Other HRR-related

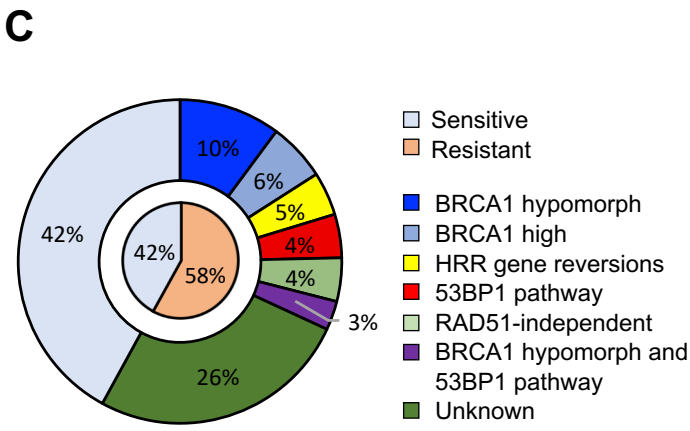
C
10%
6%
5%
4%
4%
3%
26%
42%
42%
58%
Sensitive
Resistant
BRCA1 hypomorph
BRCA1 high
HRR gene reversions
53BP1 pathway
RAD51-independent
BRCA1 hypomorph and 53BP1 pathway
Unknown

Figure 7

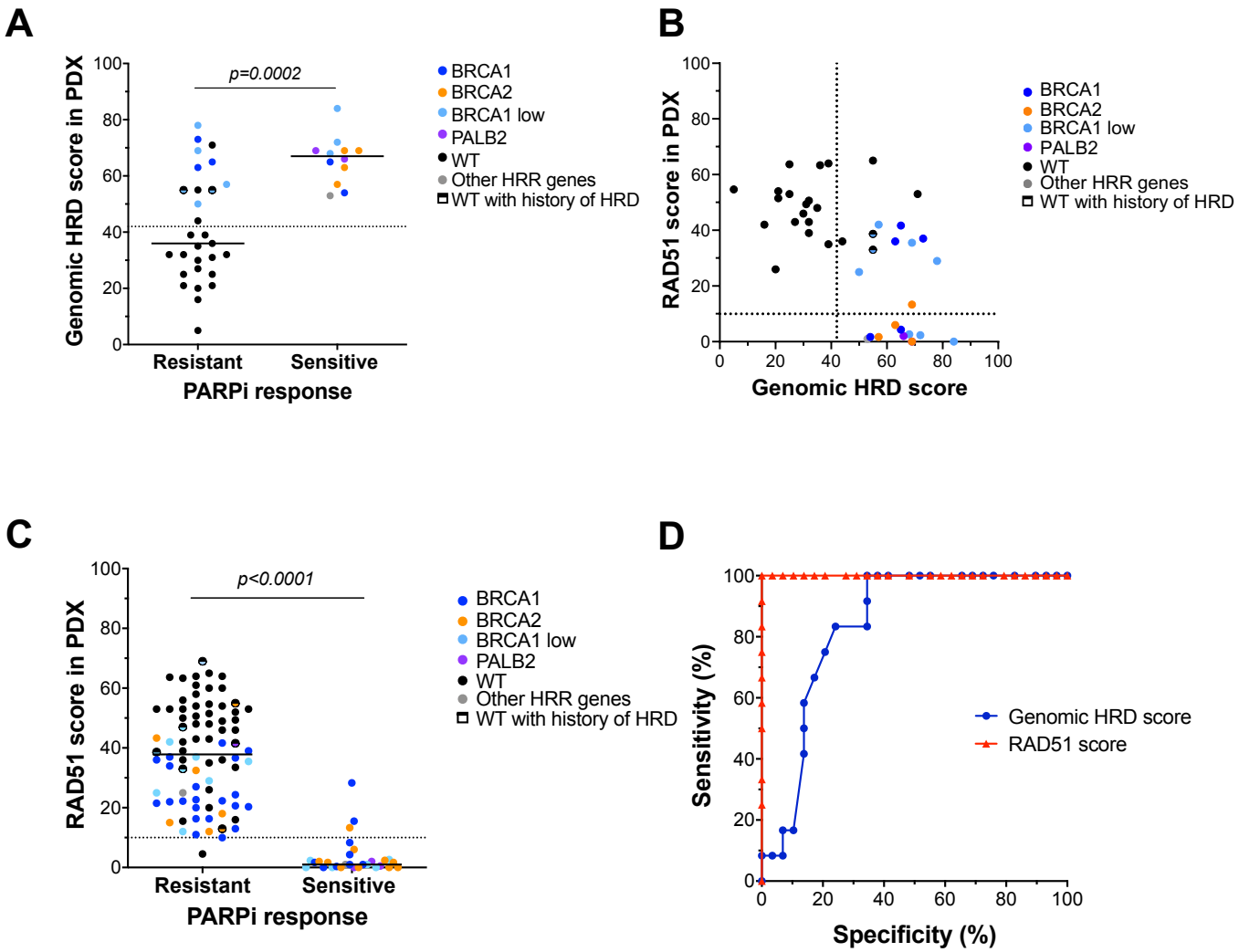
A
p=0.0002
Genomic HRD score in PDX
Resistant
Sensitive
PARPi response
BRCA1
BRCA2
BRCA1 low
PALB2
WT
Other HRR genes
WT with history of HRD
B
RAD51 score in PDX
Genomic HRD score
C
p<0.0001
RAD51 score in PDX
D
Sensitivity (%)
Specificity (%)
Genomic HRD score
RAD51 score

Figure 8

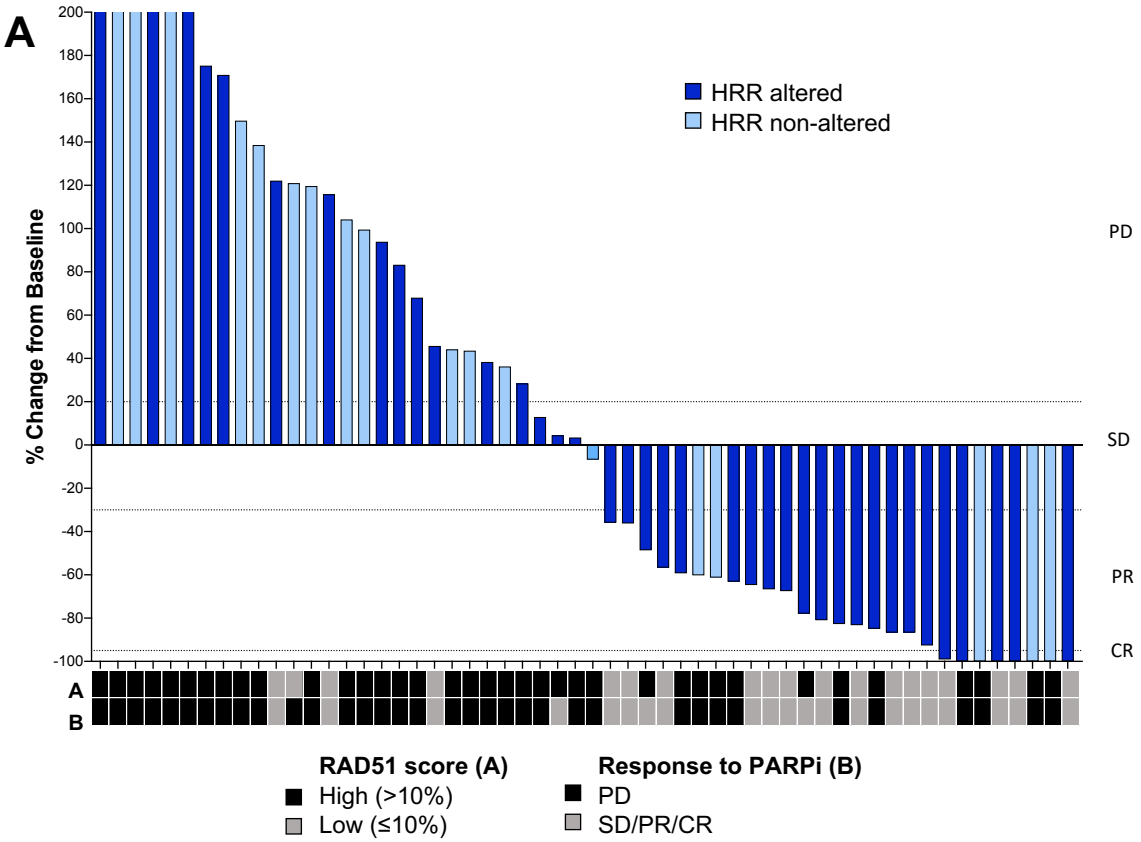
A
HRR altered
HRR non-altered
% Change from Baseline
200
180
160
140
120
100
80
60
40
20
0
-20
-40
-60
-80
-100
PD
SD
PR
CR
A
B
RAD51 score (A)
High (>10%)
Low (≤10%)
Response to PARPi (B)
PD
SD/PR/CR

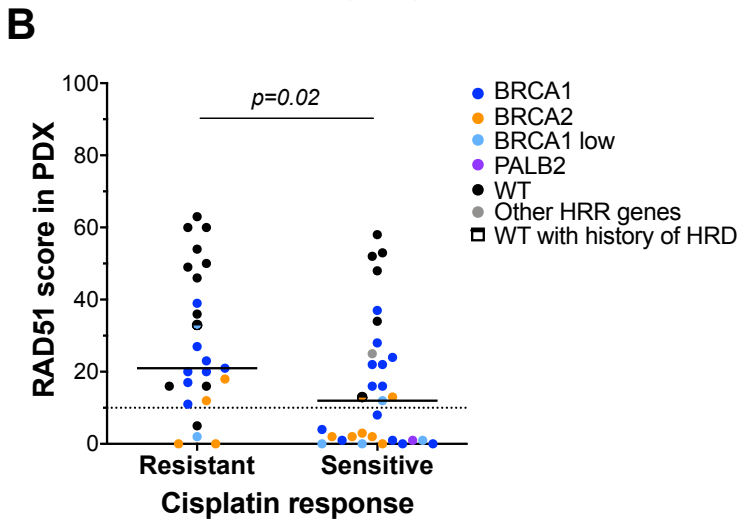
B
p=0.02
RAD51 score in PDX
100
80
60
40
20
0
Resistant
Sensitive
Cisplatin response
BRCA1
BRCA2
BRCA1 low
PALB2
WT
Other HRR genes
WT with history of HRD

Figure 9

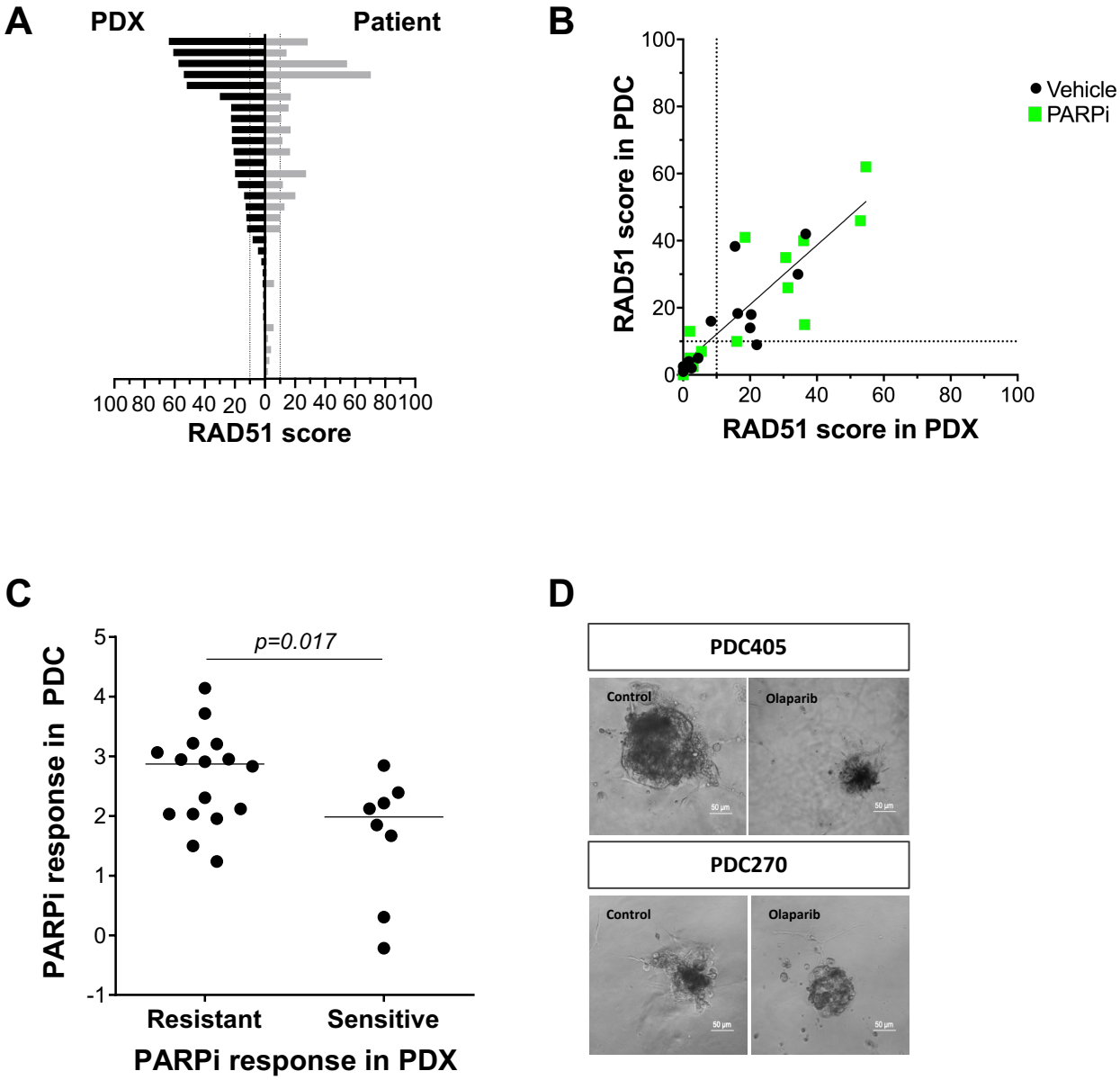
A
PDX
Patient
100 80 60 40 20 0 20 40 60 80 100
RAD51 score
B
RAD51 score in PDC
RAD51 score in PDX
Vehicle
PARPi
C
p=0.017
PARPi response in PDC
Resistant
Sensitive
PARPi response in PDX
D
PDC405
Control
Olaparib
PDC270
Control
Olaparib

Figure 10

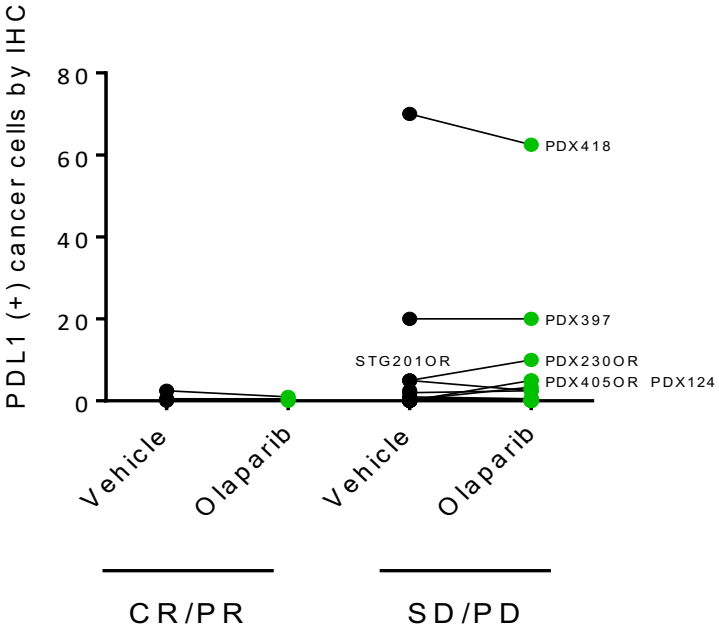
PDL1 (+) cancer cells by IHC
80
60
40
20
0
PDX418
PDX397
STG201OR
PDX230OR
PDX405OR
PDX124
Vehicle
Olaparib
Vehicle
Olaparib
CR/PR
SD/PD

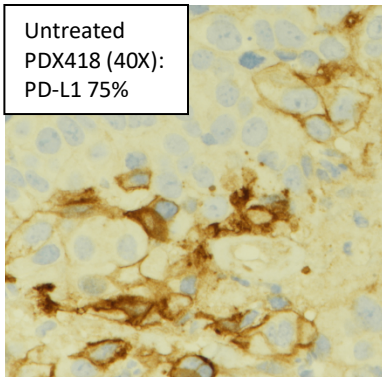
Untreated
PDX418 (40X):
PD-L1 75%

Figure 11

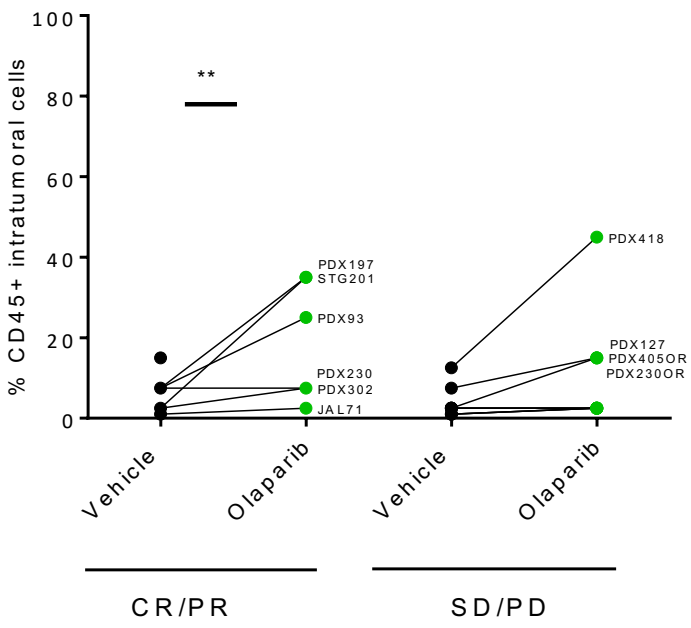
100
80
60
40
20
0
% CD45+ intratumoral cells
**
PDX197
STG201
PDX93
PDX230
PDX302
JAL71
PDX418
PDX127
PDX405OR
PDX230OR
Vehicle
Olaparib
Vehicle
Olaparib
CR/PR
SD/PD

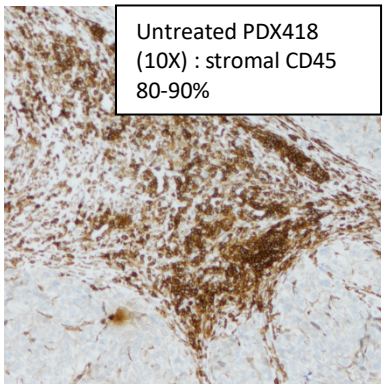
Untreated PDX418
(10X) : stromal CD45
80-90%

Figure 12

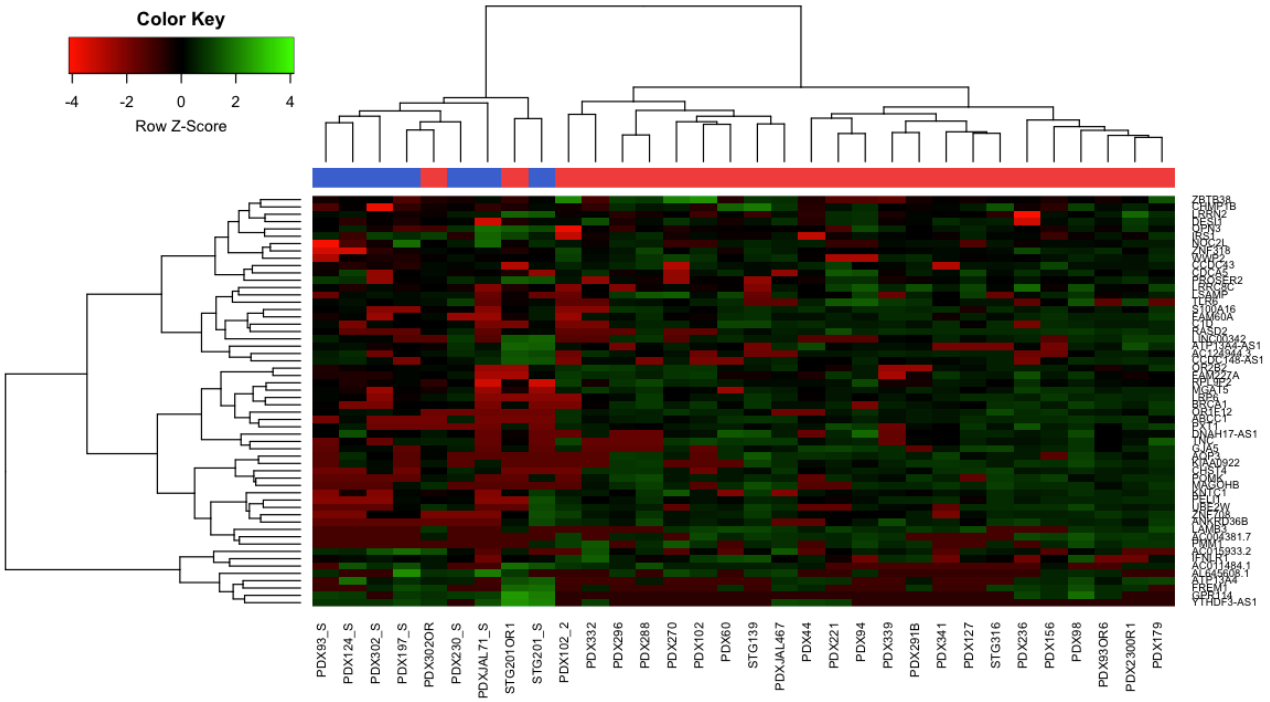
Color Key
-4
-2
0
2
4
Row Z-Score
PDX93_S
PDX124_S
PDX302_S
PDX197_S
PDX302OR
PDX230_S
PDXJAL71_S
STG201OR1
STG201_S
PDX102_2
PDX332
PDX296
PDX288
PDX270
PDX102
PDX60
STG139
PDXJAL467
PDX44
PDX221
PDX94
PDX339
PDX291B
PDX341
PDX127
STG316
PDX236
PDX156
PDX98
PDX93OR6
PDX2300R1
PDX179

Figure 13

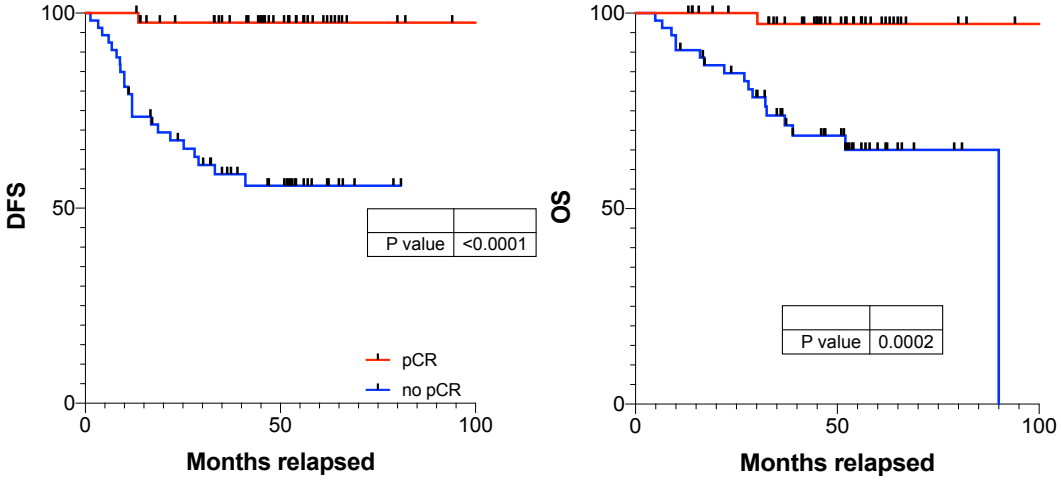
DFS
100
50
0
0
50
100
Months relapsed
P value
<0.0001
pCR
no pCR
OS
100
50
0
0
50
100
Months relapsed
P value
0.0002

Figure 14

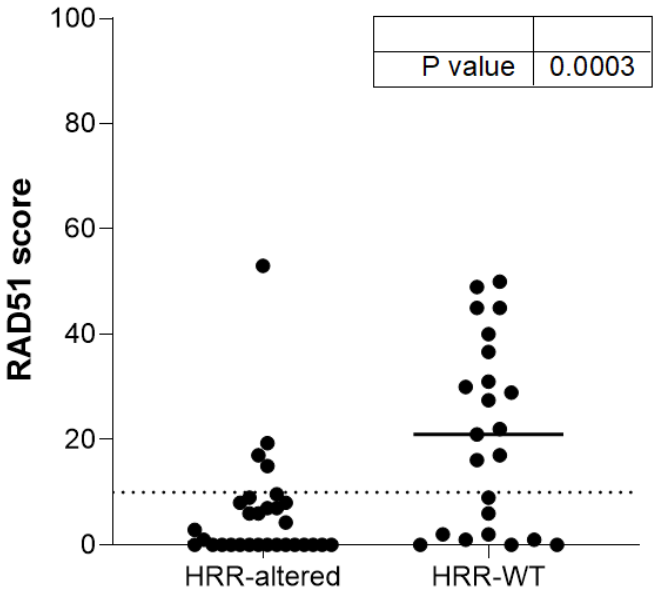

Figure 15

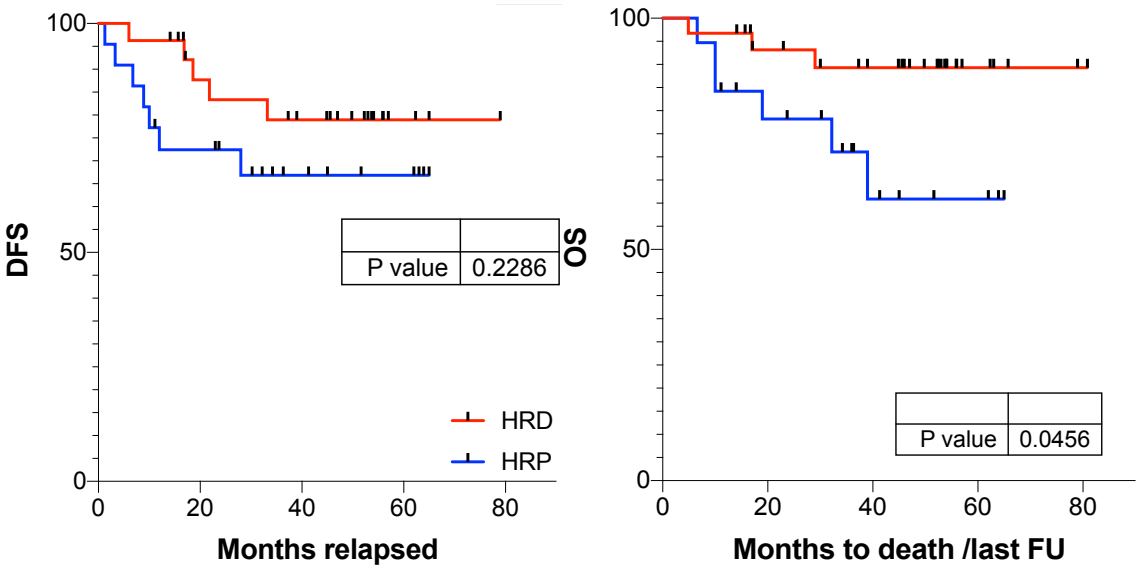
100
50
0
DFS
P value
0.2286
HRD
HRP
0
20
40
60
80
Months relapsed
100
50
0
OS
P value
0.0456
0
20
40
60
80
Months to death /last FU

Figure 16

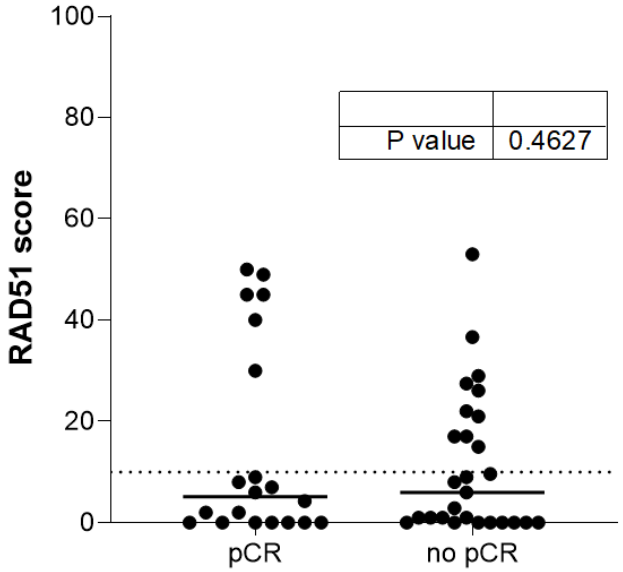

Figure 17

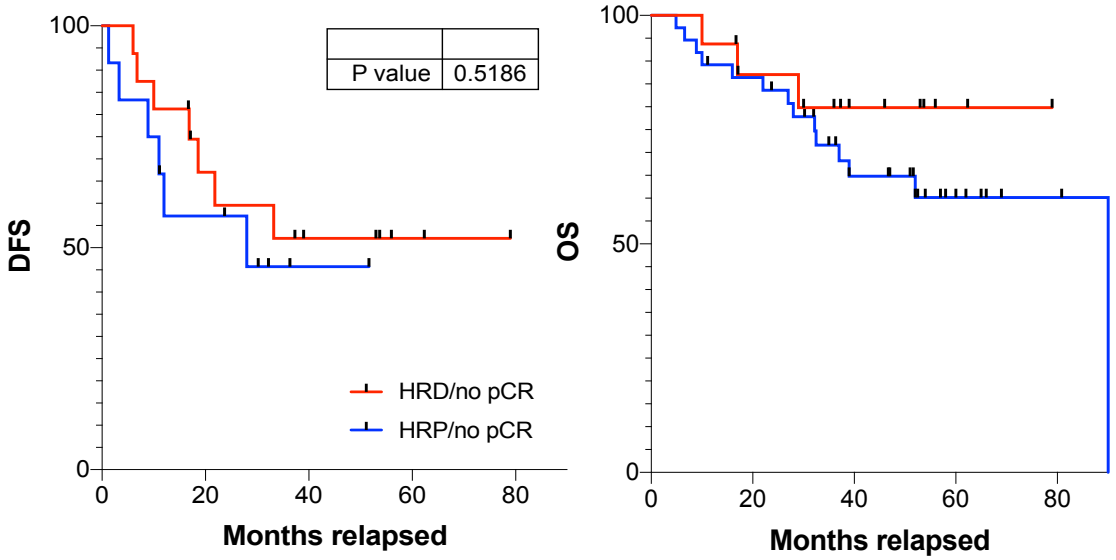
DFS
100
50
0
0
20
40
60
80
Months relapsed
P value
0.5186
HRD/no pCR
HRP/no pCR
OS
100
50
0
0
20
40
60
80
Months relapsed

Figure 18

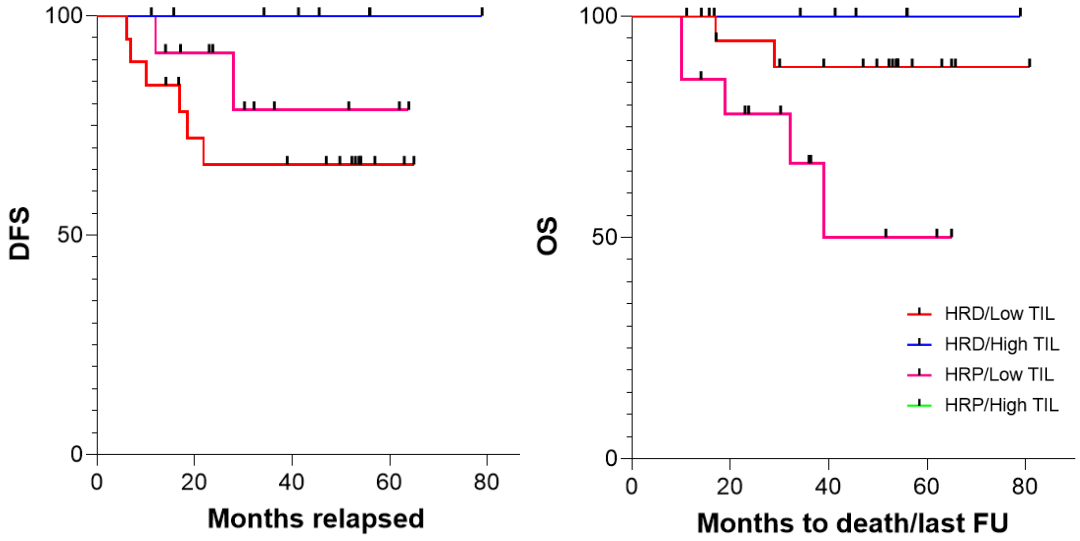
DFS
100
50
0
0
20
40
60
80
Months relapsed
OS
100
50
0
0
20
40
60
80
Months to death/last FU
HRD/Low TIL
HRD/High TIL
HRP/Low TIL
HRP/High TIL

Figure 19

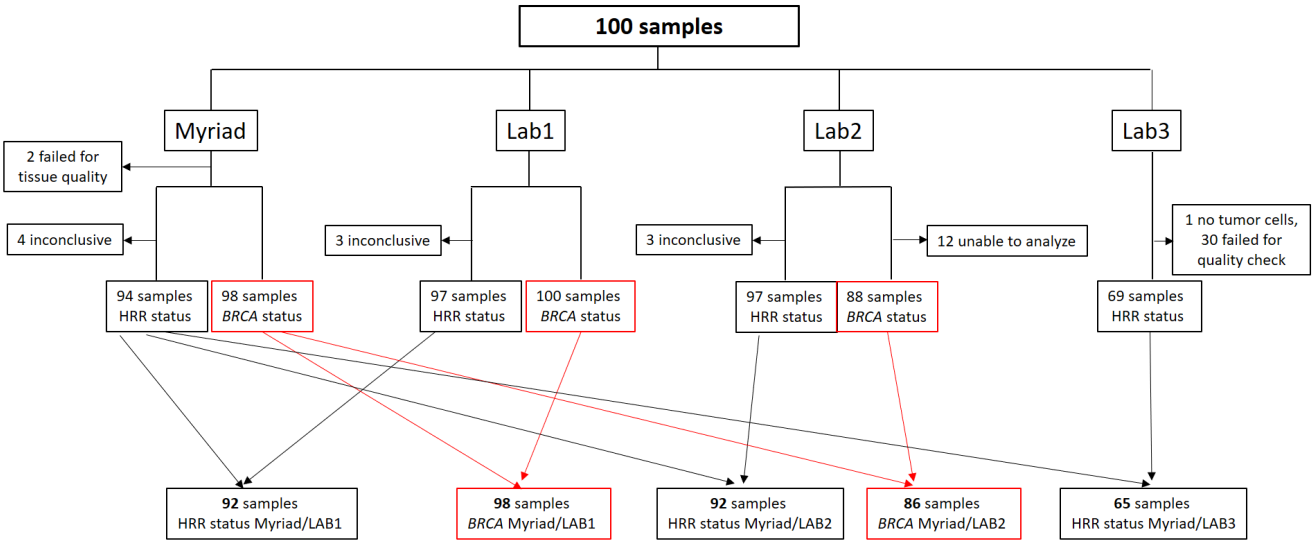
100 samples
Myriad
Lab1
Lab2
Lab3
2 failed for tissue quality
4 inconclusive
3 inconclusive
3 inconclusive
12 unable to analyze
1 no tumor cells, 30 failed for quality check
94 samples HRR status
98 samples BRCA status
97 samples HRR status
100 samples BRCA status
97 samples HRR status
88 samples BRCA status
69 samples HRR status
92 samples HRR status Myriad/LAB1
98 samples BRCA Myriad/LAB1
92 samples HRR status Myriad/LAB2
86 samples BRCA Myriad/LAB2
65 samples HRR status Myriad/LAB3

Figure 20

a) Progression free survival by status HRR Myriad

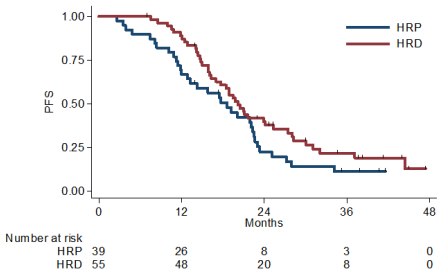

Number at risk

HRP	39	26	8	3	0
HRD	55	48	20	8	0

b) Progression free survival by status HRR LAB 1

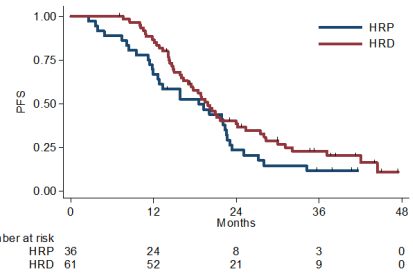

Number at risk

HRP	36	24	8	3	0
HRD	61	52	21	9	0

c) Progression free survival by status HRR LAB 2

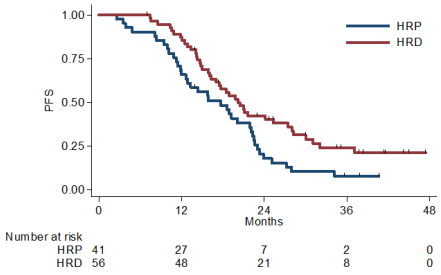

Number at risk

HRP	41	27	7	2	0
HRD	56	48	21	8	0

d) Progression free survival by status HRR LAB 3

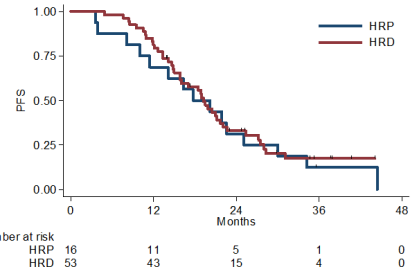

Number at risk

HRP	16	11	5	1	0
HRD	53	43	15	4	0

Figure 21

a) Overall survival by status HRR Myriad

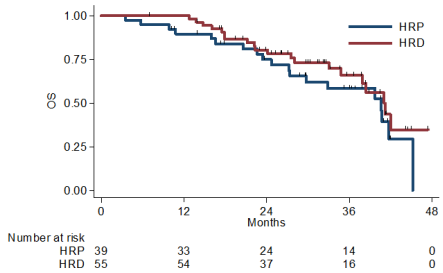

Number at risk

HRP	39	33	24	14	0
HRD	55	54	37	16	0

b) Overall survival by status HRR LAB 1

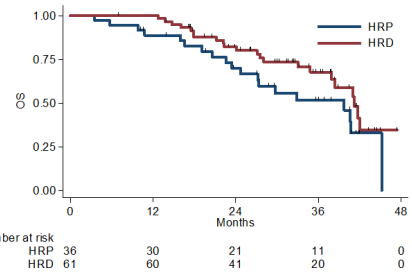

Number at risk

HRP	36	30	21	11	0
HRD	61	60	41	20	0

c) Overall survival by status HRR LAB 2

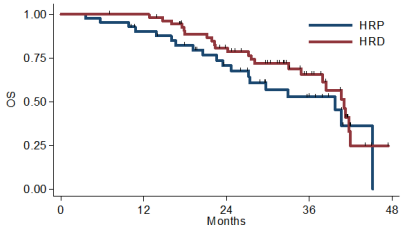

Number at risk

HRP	41	35	23	11	0
HRD	56	55	39	18	0

d) Overall survival by status HRR LAB 3

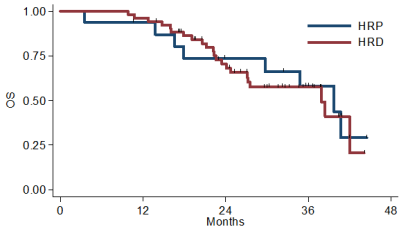

Number at risk

HRP	16	14	10	4	0
HRD	53	51	30	12	0

Figure 22

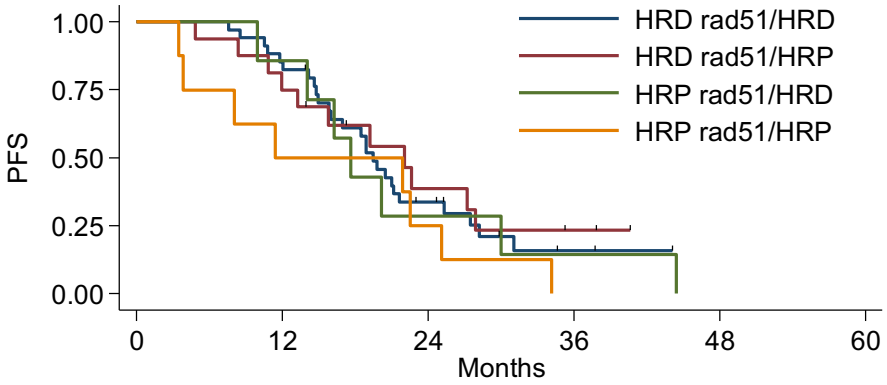

Number at risk						
HRD rad51/HRD	34	29	10	2	0	0
HRD rad51/HRP	16	12	5	2	0	0
HRP rad51/HRD	7	6	2	1	0	0
HRP rad51/HRP	8	4	2	0	0	0